npj | vaccines

Article

Published in partnership with the Sealy Institute for Vaccine Sciences

https://doi.org/10.1038/s41541-024-01046-0

SPA14 liposomes combining saponin with fully synthetic TLR4 agonist provide adjuvanticity to hCMV vaccine candidate

Ernesto Luna[1,4], Sophie Ruiz[2,4], Marie Garinot[2,4], Cyril Chavagnac[2], Pankaj Agrawal[1], John Escobar[1], Laurent Revet[2], Marie-Jeanne Asensio[2], Fabienne Piras[2], Francis G. Fang[3], Donald R. Drake III[1], Bachra Rokbi[2], Daniel Larocque[2] & Jean Haensler[2]

In the aim of designing and developing a novel saponin-based adjuvant system, we combined the QS21 saponin with low microgram amounts of the fully synthetic TLR4 agonist, E6020, in cholesterol-containing liposomes. The resulting adjuvant system, termed SPA14, appeared as a long-term stable and homogeneous suspension of mostly unilamellar and a few multilamellar vesicles, with an average hydrodynamic diameter of 93 nm, when formulated in citrate buffer at pH 6.0-6.5. When compared in an in vitro human innate immunity construct to AS01B, the QS21/MPL® liposomal adjuvant system of GSK, and with QS21-Liposomes used as benchmarks, SPA14 displayed the strongest immunostimulatory potential based on antigen-presenting cell (APC) activation and cytokine secretion, which was essentially driven by the highly active E6020 agonist in this assay. When tested as an adjuvant in vivo with human cytomegalovirus glycoprotein B (gB) and pentamer complex (PC) as test antigens, SPA14 was generally well tolerated and as active as AS01B for the induction of long-lasting CMV-neutralizing antibodies in mice and non-human primates (NHPs). Both adjuvants promoted the induction of Th-1 responses based on IgG2c production in mice and IFN-γ production in mice and NHPs, but in mice, a higher level of Th-2 cytokines (IL-5) and higher IgG1 over IgG2c secreting cells ratios were obtained with SPA14 indicating that the adjuvant profile of SPA14 could be less Th-1 biased than that of AS01B. From a developability standpoint, SPA14 could be manufactured by a simple and scalable ethanol injection method, owing to the high solubility in ethanol of all its lipidic components, including E6020. Furthermore, E6020 is a single molecule, well-characterized fully synthetic TLR4 agonist constructed in eight synthetic steps from entirely crystalline starting materials and intermediates via an optimized high-yield synthetic route. Overall, our data suggest that SPA14 is a viable, easy-to-manufacture, potent novel adjuvant system that could be broadly applicable as a ready-to-mix adjuvant in the form of a long-term stable liquid formulation.

Although several new adjuvants have been licensed as part of human vaccines over the last two decades[1], there remains a critical need for safe and potent vaccine adjuvants as highlighted by the development of several, and the licensing of at least three, adjuvanted SARS-CoV2 vaccines comprising novel adjuvants during the Covid-19 crisis[1]: Nuvaxovid®/Covovax® (Novavax), Covaxin® (Bharat Biotech) and Covax-19®/SpikoGen® (Vaxine Pty/CinnaGen) [see also: https://www.who.int/publications/m/item/draft-landscape-of-covid-19-candidate-vaccines].

The development of adjuvants that activate multiple innate immune pathways could improve the quality of vaccine immune response and protection against infectious diseases. To contribute to the development of precision adjuvants displaying specific immunological features, a new adjuvant system termed SPA14 was prepared by combining the *Quillaria Saponaria* (QuilA) saponin extract QS21[2,3] with E6020, a fully synthetic toll-like receptor (TLR) 4 agonist[4], in a cholesterol-containing liposomal delivery system. SPA14 shares some common features with AS01, the adjuvant

[1]Sanofi Vaccines business unit, R&D, Orlando, FL, USA. [2]Sanofi Vaccines business unit, R&D, Marcy L'Etoile, France. [3]Eisai Inc, Cambridge, MA, USA. [4]These authors contributed equally: Ernesto Luna, Sophie Ruiz, Marie Garinot. e-mail: jean.haensler@sanofi.com

system that is present in the highly potent shingles vaccine, Shingrix® (GSK)[5]. AS01 is a unique combination of QS21 and monophosphoryl Lipid A (MPL®), a defined detoxified product comprising several components containing 3-6 acyl chains derived from the LPS of *Salmonella minnesota* and displaying a unique immunostimulatory profile through interactions with TLR4[6–9]. In AS01, QS21 and MPL® are formulated in dioleoyl phosphatidylcholine (DOPC) / cholesterol liposomes[10,11]. The liposomal formulation was found to be important for the attenuation of QS21 cytolytic effects since it was found that saturation of QS21 with cholesterol could inhibit its hemolytic activity and improve local reactogenicity upon intramuscular injection[12,13]. Furthermore, during the clinical development of GSK's adjuvanted malaria vaccine, Mosquirix®, the MPL® plus QS21 combination in liposomes (AS01) outperformed the same combination formulated in an emulsion (AS02) in terms of safety and efficacy[14,15].

Our goal was to design a novel adjuvant system that would i) display a robust immunostimulatory profile and induce strong and long-lasting antibody responses when used with a protein vaccine, ii) would be stable and easy to manufacture for large-scale production, and iii) would be compatible with stockpiling to enable mixing with an antigen at the point of injection. For this purpose, we evaluated a formulation of QS21 in combination with E6020 in a liposome-based adjuvant system (SPA14). E6020 is a fully synthetic compound capable of mimicking precise aspects of the biological properties of natural Lipid A derived from gram(-) bacteria[4]. E6020 has a stereochemically and functionally optimized structure wherein a crystalline urea ethanolamine moiety replaces the natural di-saccharide scaffold of Lipid A. E6020 had been shown to trigger the release of innate chemokines and cytokines in mice and cultured human peripheral blood mononuclear cells (PBMCs) and dendritic cells (DCs) through TLR4 ligation and to display adjuvant effects when tested with several antigens and delivery systems in different animal models[4,16–23]. Moreover, the synthetic route to E6020 has been optimized as to synthesize the compound in high yields in no more than eight steps. Thus, the use of Eisai's well-defined fully synthetic TLR4 agonist E6020, with its distinct immunostimulatory profile, offered interesting possibilities from both the adjuvant design and the product development perspectives.

In this report we describe the manufacturing of SPA14 by using a scalable ethanol injection technique[24–26] that was made possible by the solubility of E6020 in ethanol. Formulation conditions enabling long-term colloidal and chemical stability of the SPA14 adjuvant were established. Then, we highlight detectable differences in the adjuvant profile of SPA14 compared to AS01B and QS21 liposomes when tested in vitro by using the innate Peripheral Tissue Equivalent (PTE) module of the MIMIC® system[27] and in mice when tested with a human cytomegalovirus (hCMV) vaccine candidate composed of a mixture of recombinant glycoprotein B (gB) plus pentamer complex (PC) from hCMV. Finally, we characterize the adjuvant effect of SPA14 in non-human primates (NHPs) by using the same antigen model.

Results

Manufacturing of SPA14 by a scalable ethanol injection process and characterization of the liposomal formulation

For the manufacturing of SPA14, a simple ethanol injection process was explored in the aim of keeping the industrial development timelines and costs as low as possible. At the research and pilot scale, E6020-Liposomes were prepared by solubilizing E6020 with DOPC and cholesterol in ethanol and injecting the resulting solution into an excess of stirred water or aqueous buffer by using a syringe pump. A preliminary step consisted in testing the solubility of E6020 in ethanol, which was done by using nephelometry to follow the appearance and increase of opalescence due to insolubility. When increasing the concentration of E6020 from 0.5 to 10 mg/mL in ethanol, the solution remained perfectly clear, indicative of solubility. Conversely, when MPLA was used instead of E6020, opalescence (insolubility) was observed starting at 0.5 mg/mL and increasing with the concentration of MPLA (Fig. 1b). Next, we conducted a pre-formulation study for the selection of an aqueous buffer allowing long term stability of the liposomal adjuvant in liquid form. For this purpose, SPA14 was prepared as described in the Methods section by injecting the lipids into water and adding QS21 diluted in different buffers prior to sterile filtration. Since instability of QS21 at neutral or basic pH was well-documented in the literature[28], the study used slightly acidic buffers, including PBS pH 6.0, PBS pH 6.5 and CBS pH 6.5. The study was performed in the presence of residual ethanol from the manufacturing process (2.5% in the final product; representing the worst case), but a sample dialyzed against PBS pH 6.5 to remove the residual ethanol was also included for comparison. Aliquots from the different preparations were then placed under nitrogen in type I borosilicate glass vials capped with a rubber stopper and aluminum caps and incubated at 5 °C, 25 °C, 37 °C and 45 °C. The results shown on Supplementary Fig. 1 indicated that the particle size of SPA14 liposomes was essentially unaffected by the buffer composition but heat stability of liposomal QS21 was best in PBS pH 6.0 and in CBS pH 6.5 while that of liposomal E6020 was clearly improved in CBS pH 6.5. It seemed also that residual ethanol removal by dialysis could have a beneficial effect on the stability of both QS21 and E6020. Hence, we decided to formulate SPA14 in CBS at a pH comprised between 6.0 and 6.5 and to systematically dialyze the liposomes to remove ethanol traces by following the procedure detailed in the Methods section. A typical SPA14 lot manufactured under these conditions was found to contain mostly unilamellar vesicles, mixed with a few multilamellar ones, all in the 50-150 nm size range as shown by cryo-transmission electron microscopy (Fig. 1c). The particle sizes were confirmed by DLS measurements with a Z-average of 93 nm and a PDI of 0.103. Later, the particle size specifications were set to 90 ± 30 nm with a PDI < 0.200. These product characteristics validated the use of "ethanol injection" for the manufacturing of SPA14.

Next, we tested SPA14 for its hemolytic activity by using an erythrocyte lysis assay (Fig. 1d), as previously described[12]. We confirmed that SPA14 was essentially devoid of hemolytic activity while free QS21 was strongly hemolytic in this assay, confirming that the hemolytic activity of QS21 could be quenched by incorporation into cholesterol containing E6020-liposomes.

High doses of SPA14-20 induced a differential innate immune activation in the MIMIC® PTE module compared to SPA14-8 and AS01B

Innate immune activation has been described to set the tone of adaptive immune response to vaccines and adjuvants. However, excessive activation of this immune compartment has been associated with inflammation and reactogenicity both in preclinical and clinical studies[29]. APC activation, cytokine secretion and other secreted factors, such as prostaglandin E2 (PGE2) have been suggested as in vitro surrogate biomarkers for vaccine potency and reactogenicity[30–32]. We have compared innate immune activation induced by SPA14 and its TLR4 agonist component, E6020, to that induced by AS01B (retrieved from a commercial package of Shingrix) and MPLA by using the innate peripheral tissue equivalent (PTE) module of the MIMIC® system[27,33]. Note that, in this assay, MPLA was used as a surrogate for MPL® that is comprised in AS01B and may display some differences in composition and activity[9]. Cells from MIMIC®-PTE cultures treated with the different test items shown in Table 1 were harvested 48-hours after treatment for viability, cell differentiation and activation analysis as described in Methods.

While all doses from the curve were evaluated in the MIMIC system (see Supplementary Table 1), for Fig. 2, we selected the dose dilution of 1:40 for SPA14 and 1:20 for AS01B. This was done to normalize and compare the same concentration of DOPC-Chol-QS21 between the three adjuvant formulations (Table 1). Controls were also aligned with dilution of formulated adjuvants, E6020 (200 ng/mL corresponding to a 1:40 dilution of SPA14), and MPLA (5000 ng/mL corresponding to a 1:20 dilution of AS01B). L + R (LPS + R848) was included as a standard assay positive control. Note that the lower doses selected for E6020 versus MPLA in this assay comes from preliminary testing in our laboratory, indicating that E6020 would be 10-100-fold more potent than MPLA for the activation of human DCs in vitro[22]. From the set of analytes evaluated in the study, results reported in

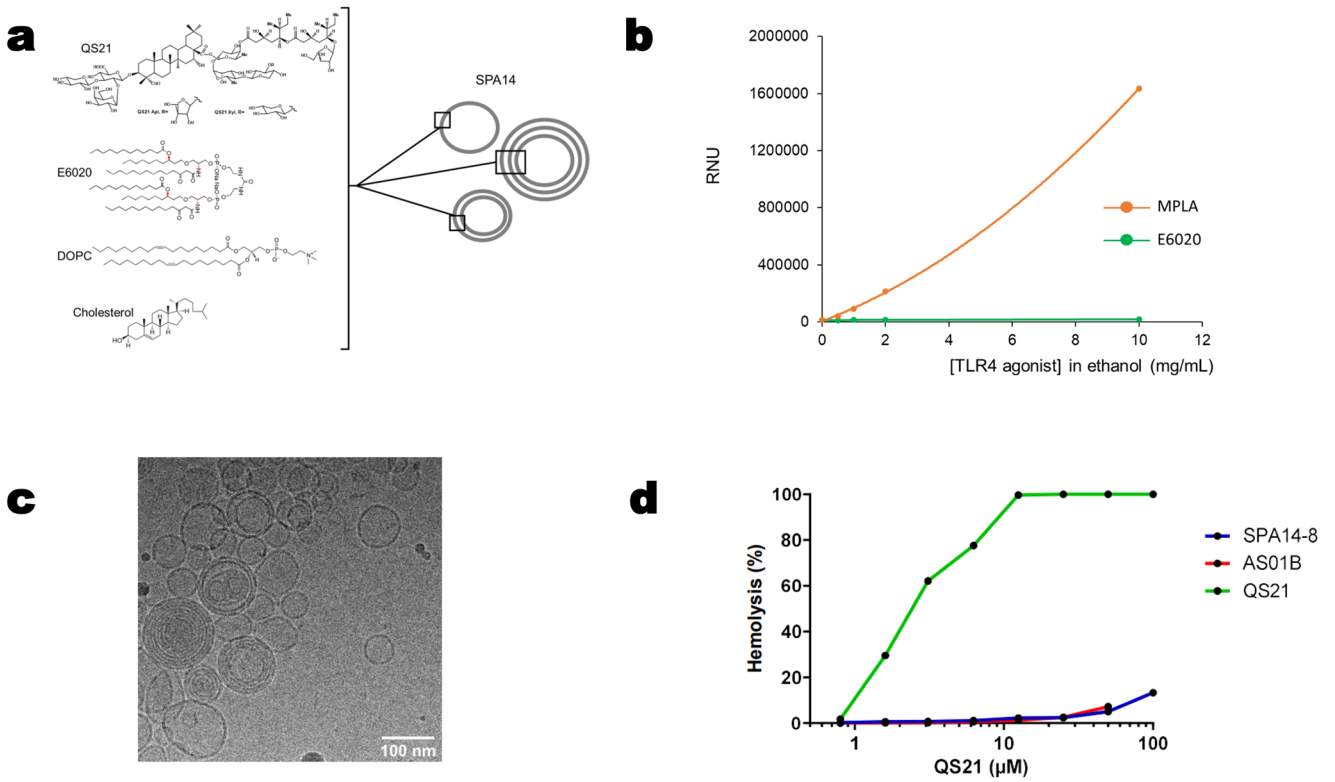

Fig. 1 | Physico-chemical characterization of SPA14 adjuvant. a Schematic view of chemical structure of SPA14 liposomes formed by DOPC, cholesterol, QS21 and E6020 consisting of a hexa-acylated acyclic structure backbone. **b** Solubility of E6020 and MPLA in ethanol. E6020 and MPLA (Sigma) powders were suspended at 0.5, 1.0, 2.0 and 10 mg/mL in absolute ethanol and solubilization was followed by nephelometry as described in the Methods section. The RNU (Relative Nephelometry Unit) of each sample was recorded and plotted on the graph. **c** Cryo EM micrograph for SPA14-20 (scale = 100 nm) with unilamellar and few multi-lamellar vesicles. **d** Hemolytic activity of QS21 and quenching of hemolysis in SPA14 and AS01B. The graph shows hemolysis of sheep erythrocytes incubated with increasing concentrations of QS21 either in free form (solution in CBS pH 6.3; green line) or formulated in SPA14-8 (blue line) or in AS01B (red line).

Table 1 | Adjuvants evaluated in the MIMIC® PTE module

Test item	Composition (mg/mL)				TLR4 agonist concentration (ng/mL) after dilution in MIMIC®-PTE			
	DOPC	Chol	QS21	TLR4 agonist	1 :20	1 :40	1 :80	1 :160
SPA14-8	4	1	0.2	0.008 (E6020)	400	200[a]	100	50
SPA14-20	4	1	0.2	0.02 (E6020)	1000	500	250	125
AS01B	2	0.5	0.1	0.1 (MPL®)	5000[a]	2500	1250	625

[a]Unformulated TLR-4 agonists, E6020 and MPLA (Invivogen), were as well tested at these specific concentrations in the assay.

Fig. 2 include cell viability (Fig. 2a), CD86+ cells percentage (Fig. 2b), IL-6 secretion (Fig. 2c), PGE2 secretion (Fig. 2d) and level of surface marker expression (Fig. 2e).

First, cell viability is critical to establish the potential immunocytotoxic effects of compounds in cellular subpopulations when in vitro systems are employed[34]. The cell viability upon each treatment condition was represented in Fig. 2a. All three formulated adjuvants (SPA14-20, SPA14-8 and AS01B) minimally reduced cell viability by 13%-18%. Hence, despite containing a higher dose of E6020, SPA14-20 did not adversely affect cell viability at the dose tested here and was comparable to SPA14-8. AS01B, the licensed adjuvant control, performed similarly to SPA14-20 and SPA14-8. When unformulated TLR4 agonists were analyzed, E6020 significantly reduced cell viability to 53% (t-test, $p < 0.0001$) while MPLA did not trigger this effect. On the other hand, LPS + R848, the positive assay control, induced a ~60% reduction in cell viability, indicating the assay was operating within specifications. The non-reduction ($p > 0.05$) in cell viability induced by the liposomal vehicle (DOPC/cholesterol/QS21) suggests a major role of liposome vehicle mitigating the immunocytotoxicity potential of E6020. Based on this viability data, E6020 appears to be more cytotoxic than MPLA in the MIMIC assay, however, this cytotoxic effect appears to be largely attenuated upon formulation of E6020 into SPA14 liposomes. Results from the nonclinical safety testing of E6020 injected alone or formulated in SPA14 have been published previously[4,35] and these results indicate that E6020 is generally well tolerated in vivo across a range of doses.

Of particular interest for an innate immune assessment is to detect an increase of conventional dendritic cells (DC) number expressing costimulatory markers. These markers together have been described as important markers of differentiated APCs and their maturation stage[36]. The expression of costimulatory markers on harvested cells is typically used to demonstrate the effect of adjuvants on APC differentiation and activation. Fig. 2b shows the percentage of CD86+ cells within HLA-DR+ CD11c+ cells as a marker of APC differentiation/maturation. The figure suggests all three TLR4-agonist-containing adjuvants induced more than 3-fold increase in the % of HLA-DR + /CD11c + /CD86+ cells (10-17%) over the mock control (~4%). Minimal differences in CD86 expression were observed between SPA14-8, SPA14-20, and AS01B, suggesting a similar capacity of SPA14-8 and SPA14-20 to induce APC differentiation in vitro relative to AS01B. In contrast, there was a certain reduction of CD86+ cells triggered by the

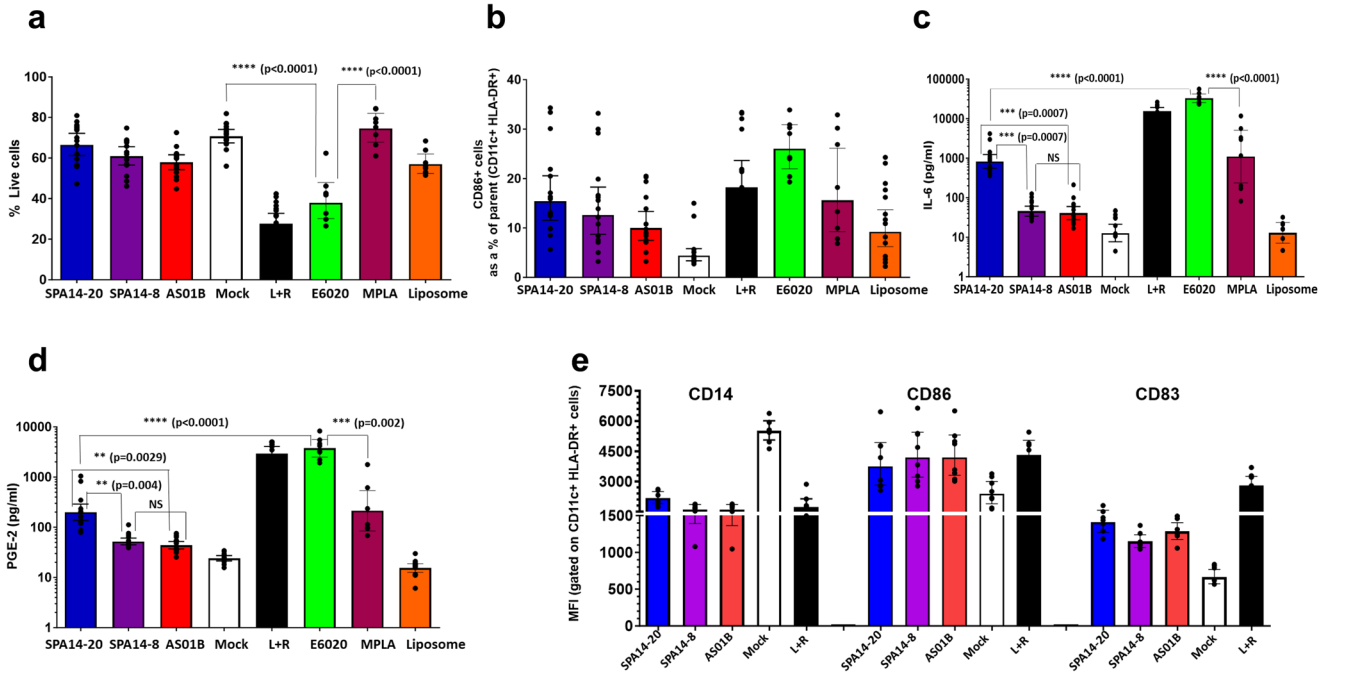

Fig. 2 | Adjuvants response in MIMIC® PTE assay. The MIMIC® PTE was treated with various human dose dilutions of adjuvants for 48 h, as described in Table 1. The cells were then harvested and evaluated for phenotype and viability by flow cytometry and cytokines by multiplex array. **a** Cell viability: % of viable cells after 48 h in MIMIC PTE assay. **b** APC differentiation was measured by the number of mature CD86+ cells as a percent of parent CD11c+ HLA DR+ cells. **c** IL-6 secretion as a representative cytokine determined in the culture supernatants by Luminex-based multiplex assay. **d** PGE-2 secretion determined by ELISA in the culture supernatants. **e** the level of surface markers (CD14, CD86 and CD83) on APCs (CD11c HLA + DR+ cells) measured by flow cytometry using specific antibodies. Data for SPA14-20, SPA14-8 and liposomes (SPA14 without E6020) at a 1:40 dilution and data for AS01B at a 1:20 dilution to normalize DOPC-Chol-QS21 contents between the 3 adjuvants are represented here. E6020 (200 ng/mL corresponding to a 1:40 dilution of SPA14), MPLA (5000 ng/mL corresponding to a 1:20 dilution of AS01B), liposomes and the L + R assay positive control were used as benchmarks in the study (see Methods). Each dot represents an individual donor and the bar represents Geometric Mean with 95% CI; $N = 8–15$ donors. Statistical comparisons were performed using GraphPad Prism by unpaired, two tailed T test for relevant conditions.

formulated TLR4 agonists (SPA14 and AS01B) compared to unformulated TLR4 agonists (11 vs 18% for MPLA and 17 vs 26% for E6020; see Supplementary Table 1). In line with the reactogenicity data, this result suggests that the liposome formulation may impede the TLR4 direct ligation on APCs, thereby reducing the differentiation of myeloid dendritic cells (mDC) expressing co-stimulatory molecules, as already suggested by others[37]. The analysis of the cell surface marker expression (Fig. 2e) by measuring the mean fluorescence intensity (MFI) per cell shows that the tested adjuvants (AS01B and SPA14) and the positive control, LPS + R848, all trigger DC maturation and activation, as indicated by the decreased expression of the monocyte marker, CD14, and increase in the surface receptor density of both CD86 and CD83.

Culture supernatants from untreated and treated MIMIC®-PTE cultures were then analyzed for cytokine/chemokine secretion using a Millipore custom 12-plex array and for PGE2 secretion by ELISA. Fig. 2c indicates that SPA14-20 induced IL-6 secretion (as an example of pro-inflammatory cytokine) to a maximum of ~800 pg/mL, which was almost 20-fold higher (unpaired t-test, $p = 0.0007$) than that induced by SPA14-8 (45.6 pg/mL) and AS01B (40.9 pg/mL), respectively. While MPLA (5 µg/mL) induced IL-6 secretion similar to that of SPA14-20, it was significantly lower than 100 ng/mL of E6020, which induced robust IL-6 production (~ 8000 pg/mL, t-test $p < 0.0001$). In fact, 100 ng/mL of free E6020 induced as high IL-6 secretion as the assay positive control (LPS + R848) and significantly higher IL-6 secretion than 100 ng/mL of E6020 formulated in SPA14-20 (t-test, $p < 0.0001$). Biostatistical analysis suggests that SPA14-20 induced more IL-6 than SPA14-8 and AS01B while, in general, SPA14-8 induced similar cytokine secretion compared to AS01B (t-test, NS). This result is aligned with PGE2 secretion (Fig. 2d): neither SPA14-8 nor AS01B strongly induced PGE2 production (~ 40-52 pg/mL) compared to the mock control (~ 24 pg/mL), while SPA14-20 induced significantly higher (200 pg/mL, t-test, $p < 0.005$) production of PGE2 than SPA14-8 and AS01B. As observed for IL-6, there appears to be an impact of liposome formulation on reducing PGE2 secretion induced by unformulated TLR4 agonists; whereas MPLA induced similar PGE2 secretion to SPA14-20, E6020 triggered 10-100-fold higher levels of PGE2 than MPLA and all formulated compounds. In general, SPA14-20 induced more PGE2 secretion than SPA14-8 and AS01B, but SPA14-8 induced a PGE2 secretion that was similar to that of AS01B. Importantly, the secretion of both IL-6 and PGE2 is likely driven by TLR4 signaling because the liposome control did not induce secretion of IL-6 or PGE2 above baseline levels in the mock control (Fig. 2c, d).

In Fig. 3, we generated a comprehensive heat map to expand innate immune readouts and further explore TLR4 signaling pathways presented in Fig. 2. TLR4 uses two distinct signaling pathways: the TIRAP/MyD88-dependent pathway is initiated at the cell membrane and elicits rapid MAP kinase and NF-κB activation, and the TRIF/TRAM pathway is initiated after endocytosis and leads to the induction of type I interferons[37]. Both pathways are relevant for TLR4-mediated dendritic cell activation and adjuvanticity. While certain studies associated inflammation with the MyD88 pathway and adjuvanticity with the TRIF pathway[38], other authors[18] demonstrated that both strong and weak TRIF-inducing TLR4 agonist adjuvants could stimulate adaptive humoral immune responses. To analyse TLR4 signaling, we separated cytokines and chemokines as being either MyD88-dependent (IL-6, IL-8, MIP-1B, IL-1B and TNFα) or TRIF-dependent (MCP-1, IP-10 and RANTES).

As a general trend, SPA14-20 induced an intermediate innate immunostimulatory profile, generating cytokine/chemokine secretion that was typically higher than that induced by SPA14-8 and AS01B but lower than that of the E6020 control. Clear differences between E6020 and MPLA were

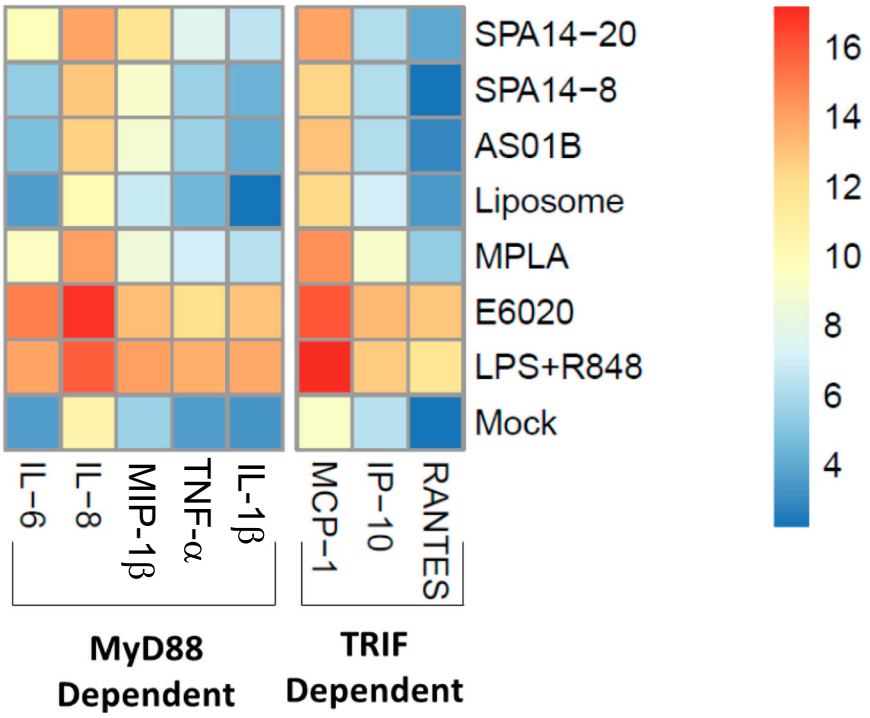

Fig. 3 | Heat map showing cytokine/chemokine responses to different adjuvants in the MIMIC® PTE assay. Data for SPA14-20, SPA14-8, and liposome at 1:40 dilution and AS01B at the 1:20 dilution are represented here as to normalize DOPC-Chol-QS21 contents in the different formulations. E6020 (200 ng/mL, corresponding to a 1:40 dilution of SPA14) MPLA (5000 ng/mL, corresponding to a 1:20 dilution of AS01B), and liposome (SPA14 without E6020 at a 1:40 dilution) were evaluated along with a LPS + R848 (L + R) positive control. Cytokines and chemokines were organized based on their alignment with the TLR4- intracellular signaling pathways, MyD88 and TRIF. $N = 8–15$ donors.

detected in the in vitro system, probably due to differences between TLR4 signaling induced by E6020 vs MPLA. This is aligned with the literature[18,22], in which E6020 induced higher cytokine secretion than MPLA analogues when compared side-by-side. It is also clear from the analysis that E6020 induced a stronger innate immune activation when tested individually versus formulated into SPA14 liposomes, despite the presence of QS21 in the liposomal formulation. In a similar manner, the innate immune activation induced by MPLA was stronger than that of AS01B in the MIMIC® PTE system. Going deeper into TLR4 signaling analysis, we observed that, in general, SPA14-20 induced higher secretion levels from the MyD88 pathway than AS01B, but, in summary, we have seen that SPA14-20 and AS01B induced both MyD88 and TRIF pathways in the innate immune activation, which could predict a good in vivo adjuvanticity.

SPA14 increased binding IgG1 and IgG2c antibodies and neutralizing antibodies to CMV-gB and PC to the same level as AS01B in mice

Based on the in vitro results and considering the good product tolerability observed during a preliminary non-clinical safety assessment conducted in rabbits[35], the adjuvants were then further compared in mice and macaques using a CMV vaccine candidate based on the combined recombinant CMV gB and PC antigen.

In C57BL/6 mice, significant adjuvant effects were observed with SPA14-20 and AS01B on BADrUL131-Y4 CMV virus neutralizing antibodies (Fig. 4a). This effect was most significant post second immunization at D35 and beyond (p value < 0.0001 compared to the non- adjuvanted group). Virus-neutralizing titers were measured on ARPE-19 epithelial cells in the absence of complement, which reflects the neutralizing activity of antibodies directed against both CMV gB and PC. Similar results were obtained with MRC-5 fibroblasts in the presence of complement, which reflects essentially the neutralizing activity of anti-CMV gB antibodies (Supplementary Fig. 2). The kinetic of the neutralizing antibody response was characterized by a significant boost effect with approximately a 100-fold increase in neutralizing antibody titers from D20 to D35. At D35, geometric mean values (GMTs) of neutralizing titers reached 3.75 Log10 with SPA14-20 and 3.98 Log10 with AS01B, whereas a GMT of 1.82 Log10 was obtained in the non-adjuvanted group. There was no significant difference between the neutralizing antibody titers measured in the SPA14-20 and AS01B groups.

The strong adjuvant effect of SPA14-20 and AS01B on CMV gB and PC also translated into a significant increase in IgG1 and IgG2c binding antibody titers specific to CMV gB (Fig. 4c, d) and PC (Fig. 4e, f) as measured by standard ELISA. IgG1 and IgG2c binding antibody curves followed the same kinetics as the neutralizing antibody curve, with a clear boosting effect after the second administration. The effect of both adjuvants was most striking on IgG2c titers with an over 1000-fold increase compared to the non-adjuvanted antigens at D35 and beyond ($p < 0.001$). IgG1 titers also increased in the adjuvanted groups but to a lesser extent (about 10-fold) compared to the non-adjuvanted group ($p < 0.01$) demonstrating a Th1-oriented response induced by both SPA14 and AS01B. As for neutralizing antibody titers, there was no significant difference between the levels of binding antibody titers measured in the SPA14-20 and AS01B groups (see also Supplementary Fig. 3 for individual responses).

Both SPA14 and AS01B induced a Th-1 adjuvant effect in C57BL/6 mice, but that of AS01B appeared to be more Th-1-biased

The frequency of IgG1 and IgG2c-secreting B cells specific to CMV gB and PC was assessed by spleen cell ELISPOT at D35 (2 weeks after the second immunization) or D179 (end of the study), after in vitro restimulation with the antigens (memory B cells) (Fig. 5). In both adjuvanted groups, the frequencies of antibody-secreting B cells (ASCs) and memory B cells specific to gB (Fig. 5a, c) and PC (Fig. 5b, d) were significantly increased over the non-adjuvanted group ($p < 0.001$). Interestingly, in the AS01B group, the frequencies of anti-gB and anti-PC IgG2c ASCs and memory B cells were significantly increased over those measured in the SPA14-20 group (respective p-values of 0.005 and 0.002) while there was no significant difference in the frequencies of IgG1 secreting B cells, except at D179 where AS01 induced more IgG1-secreting mB cells specific to gB than SPA14-20. Based on these observations, AS01B appeared as a more pronounced Th-1-biased adjuvant than SPA14.

This trend was confirmed by determining the frequency of IFN-γ and IL-5 secreting T cells specific to gB (Fig. 6a, b) and PC (Fig. 6c, d) using a Fluorospot assay on freshly isolated spleen cells from the immunized mice at D35. Results indicate that both SPA14 and AS01B induced significantly

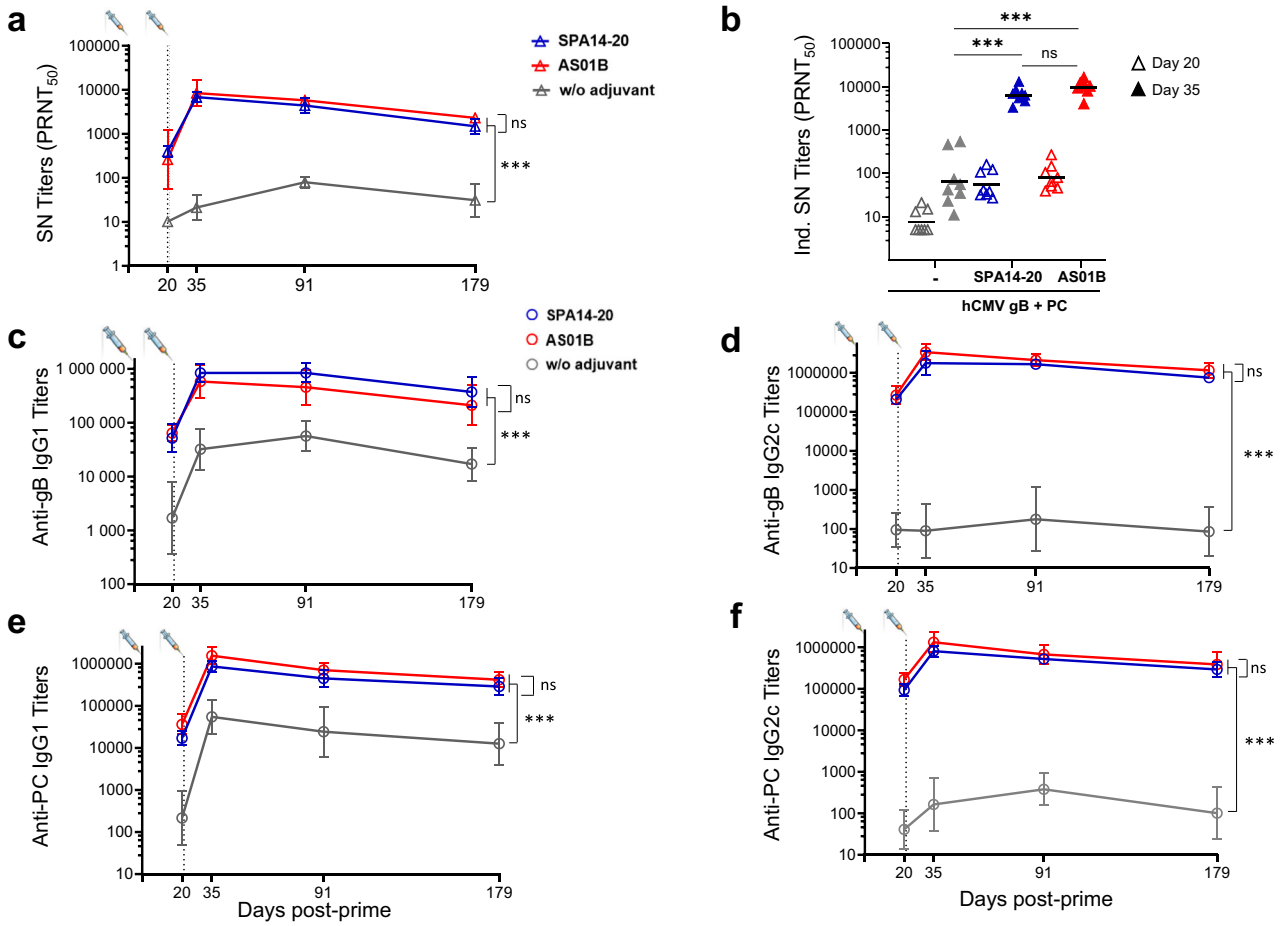

Fig. 4 | hCMV specific neutralizing and IgG response from immunized mice sera. **a** BADrUL131-Y4 CMV virus strain neutralizing titers ($PRNT_{50}$) were determined using epithelial ARPE-19 cells and represented over time. For each group, GMT and 95% CIs are represented. **b** Individual neutralizing titers at D20 (3 weeks after single immunization; open triangles) and D35 (2 weeks after the second immunization; filled triangles) shown as scattered plots with group GMTs shown as horizontal bars. **c–f** IgG1 and IgG2c antibody titers specific to CMV-gB (**c, d**) and PC (**e, f**) were determined by ELISA and reported on a (Log10) scale. For each group, GMT and 95% CIs are represented over time. Groups of mice immunized in the absence of adjuvant (○,△,▲), in the presence of SPA14-20 (○,△,▲) or AS01B (○,△,▲) are shown. Group comparisons were done by Dunnett or Tukey adjustment. We applied one-or two-way or repeated ANOVA as a function of the readout (* p value < 0.05, ** p value < 0.01, *** p value < 0.001).

higher IFN-γ-secreting cell numbers, specific to both gB and to PC compared to the non-adjuvanted group (p values ranging from $p < 0.01$ to <0.001), which is another indicator of a Th1 oriented response. No significant adjuvant effects were measured on IL-5-secreting cell numbers specific to gB but a significant reduction in the IL-5-secreting cell number specific to PC was observed in the AS01B group compared to the antigen alone and SPA14-20 groups (respective p values of $p < 0.001$ and $p < 0.05$). In this case, the increased Th-1 bias of AS01B was reflected by an increase in the IFN-γ cell number specific to gB and a decrease in the IL-5-secreting cell number specific to PC in the AS01B group compared to the antigen alone and SPA14 groups.

SPA14 had an adjuvant effect that was equivalent to that of AS01B in NHPs (cynomolgus macaques) based on B and T cell responses

The adjuvant effect of SPA14 on CMV gB and PC was further evaluated in NHPs. In this study, 5 cynomolgus macaques per group received three IM injections of 20 µg of CMV-gB plus 20 µg of CMV-PC, given either without adjuvant (control group) or in the presence of a human dose of AS01B or SPA14. For SPA14, the two formulations (i.e., SPA14-8 and SPA14-20) characterized in the MIMIC® PTE module were compared to AS01B. The immunizations were performed at D0 and D56 by IM injections under a volume of 500 µl (SPA14 and antigen alone groups) or 550 µl (AS01B group). A booster injection with the same formulations was given six months later (D189). BADrUL131-Y4 CMV virus-neutralizing antibody titers (Fig. 7a) were detected after the first dose, increased after the second dose and peaked 4 weeks after the booster injection. Antibody titers decreased at approximately the same rate across all groups, however high and durable neutralizing activities were measured over 2-years after the booster injection with geometric mean titers plateauing at around 5000 between 12 and 31 months in SPA14 and AS01B groups. SPA14 and AS01B had a clear adjuvant effect on CMV gB + PC-induced virus-neutralizing antibodies, with no significant difference between the two SPA14 formulations and AS01B. Peak geometric mean titers of serum neutralizing antibodies measured 4 weeks following the booster administration (D217) reached 431 in the non-adjuvanted group and 75673, 48206 and 62567 in the SPA14-8, SPA14-20 and AS01B groups, respectively (Fig. 7b).

Similar adjuvant effects were observed upon determination of IgG-secreting memory B cells specific to CMV gB (Fig. 7c) and PC (Fig. 7d) by B cell ELISPOT assay using fluorospot kits. In the macaques, the time course of antigen-specific memory B cells almost overlapped in the adjuvanted groups with peak levels of antigen-specific-IgG-secreting memory B cells over total IgG-secreting memory B cells reaching 20 to 70 four weeks following the booster administration (D217), representing a 16-60-fold increase over the non-adjuvanted group.

We also determined IFN-γ- or IL-4-secreting T cells specific to CMV gB (Fig. 8a, b) and PC (Fig. 8c, d) at the peak of circulating T cell

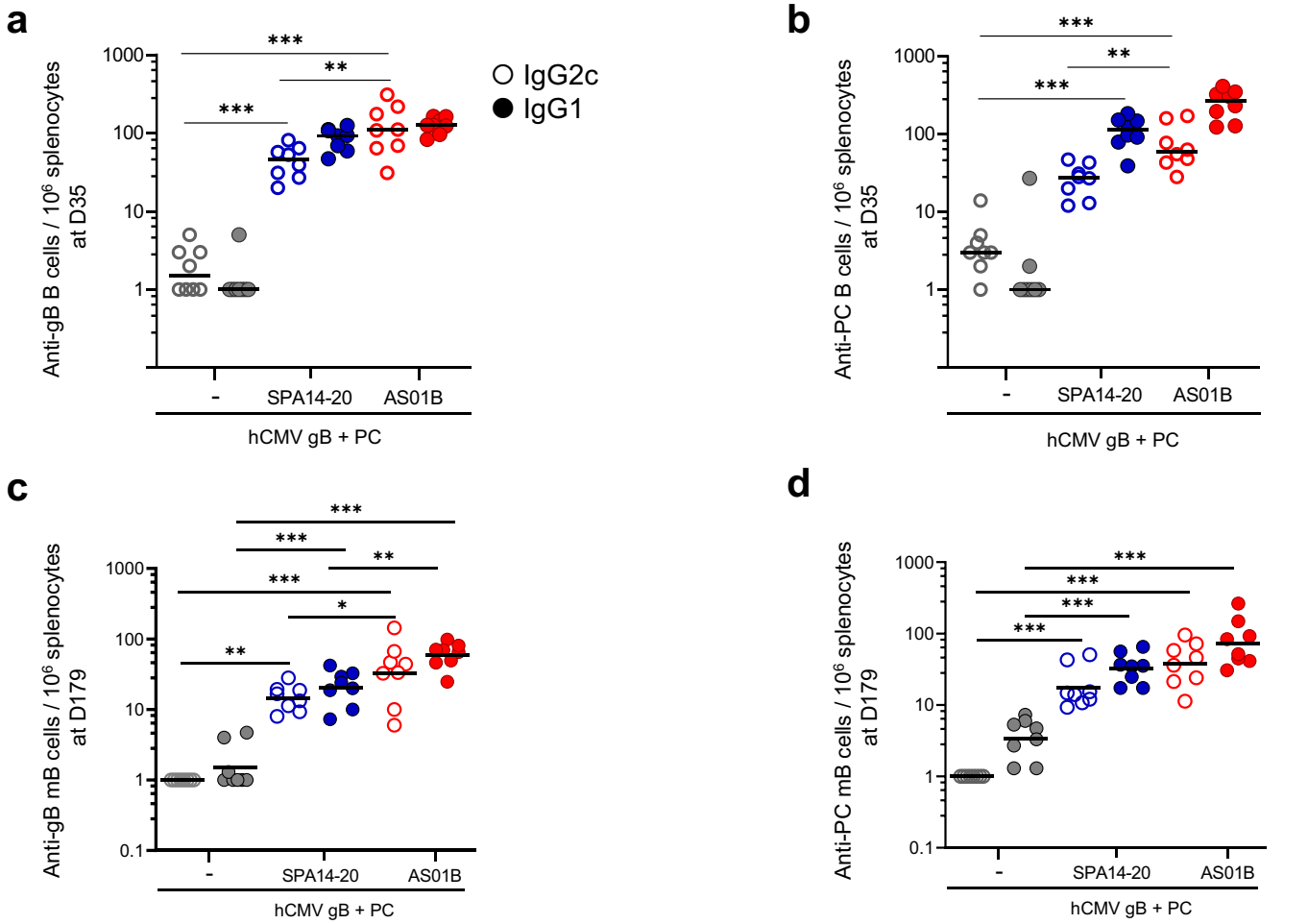

Fig. 5 | IgG2c- and IgG1-secreting B cells measured in splenocytes of immunized C57BL/6 mice at D35 and D179 (memory B cells). a, b The number of gB- and PC-specific IgG2c- and IgG1-secreting B cells per 10^6 spleen cells was determined at D35 without restimulation and **c** and **d**, at D179 after in vitro restimulation with CMV-gB or CMV-PC. Results are shown as scattered plots with group GMTs as horizontal bars. Groups of mice immunized in the absence of adjuvant (◯,●), in the presence of SPA14-20 (◯,●) or AS01B (◯,●) are shown. Open circles are for IgG2c-secreting cells and filled circles are for IgG1-secreting cells. Group comparisons were done by Tukey adjustment and one-way ANOVA (* p value < 0.05, ** p value < 0.01, *** p value < 0.001). All statistically significant differences between groups are indicated on Fig. 5. An absence of indication means that the difference did not reach statistical significance ($p > 0.05$).

responses (D197) by using a T cell ELISPOT assay on macaque PBMCs. SPA14-8 and SPA14-20 adjuvanted both the CMV-gB and PC-specific IFN-γ and IL-4 responses to similar levels, which were comparable to that of AS01B.

SPA14 was well-tolerated by immunized NHPs

From a safety standpoint, none of the immunized macaques experienced severe clinical symptoms. There was a small and short drop in normal body weight gain one week following booster administration in all groups, but the body weight gain rapidly returned to normal two weeks later (Supplementary Fig. 4a). Animals were also tested for CRP concentration in serum as a marker of inflammation following each administration. We observed a significant increase in CRP levels one-day post injection (D1) in all monkeys that received an adjuvanted vaccine, whether the adjuvant was SPA14-8, SPA14-20 or AS01B. However, the CRP levels rapidly returned to pre-immunization levels two days later (D3) (Supplementary Fig. 4b). The same trend was observed for the anti-inflammatory cytokine, IL-1RA, which tended to increase in some monkeys at D1 and returned to background levels at D3 (Supplementary Fig. 4c).

Discussion

One of the most potent adjuvant systems approved for human vaccines is AS01, a liposomal adjuvant system combining QS21 with MPL® and included in GSK's licensed vaccines Shingrix®, Arexvy® and Mosquirix®, administered respectively to prevent zoster and RSV in elderly populations[39–41], and to fight malaria in endemic countries[14,42]. AS01 also demonstrated potency in the clinical development of experimental vaccines against *Mycobacterium tuberculosis*[43], HIV[44] and CMV[45]. Our goal was to formulate a novel highly potent adjuvant system with a robust immunostimulatory profile, and which could be easily manufactured for large-scale production. For this purpose we developed a saponin-based adjuvant system by combining QS21 with liposomes comprising the well-defined fully synthetic clinical stage TLR4 agonist developed by Eisai Inc. and identified as E6020[4]. Along the same lines, others used synthetic Lipid A (SLA) in an adjuvant system termed SLA-LSQ[46], synthetic monophosphoryl 3-deacyl Lipid A (3D-PHAD®) in an adjuvant system termed ALFQ[47] or synthetic monophosphoryl 3-deacyl, hexa-acyl Lipid A (3D(6-acyl) PHAD®) in an adjuvant system termed LMQ[48]. The use of well-defined synthetic TLR4 agonists in these adjuvant systems may allow simpler production and QC methods as compared to a natural detoxified LPS extract like MPLA/MPL® and our results indicate that E6020 could work at lower doses than natural MPLA.

SPA14 liposomes were prepared by an ethanol injection process. The method was selected for simplicity and scalability, which is beneficial from an industrial development standpoint. This liposome manufacturing method has been used for instance to produce billions of doses of SARS-

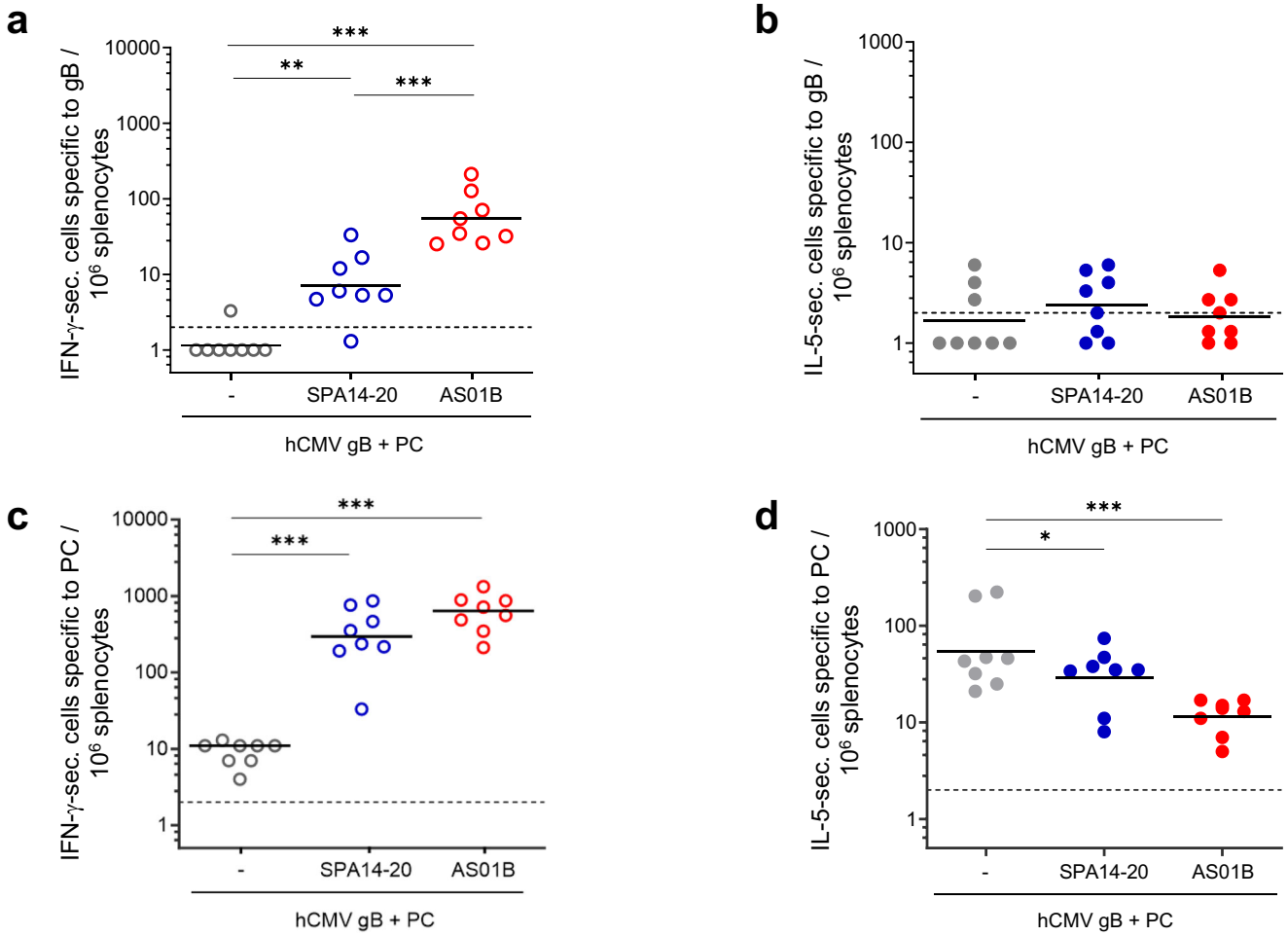

Fig. 6 | hCMV antigen specific IFN-γ- and IL-5-secreting cells measured in splenocytes of immunized C57BL/6 mice two weeks after the second immunization (D35). a, b The number of gB-specific IFN-γ- and IL-5-secreting cells and **c** and **d**, the number of PC- specific IFN-γ- and IL-5-secreting cells per 10^6 spleen cells were represented as scattered plots with group GMTs as a horizontal bar. Groups of mice immunized in the absence of adjuvant (○,●), in the presence of SPA14-20 (○,●) or AS01B (○,●) are shown. Open circles are for IFN-γ-secreting cells and filled circles are for IL-5-secreting cells. Group comparisons were done by Tukey adjustment and one-way ANOVA (* p value < 0.05, ** p value < 0.01, *** p value < 0.001). All statistically significant differences are indicated on the graph.

CoV2 mRNA vaccines formulated in lipid nanoparticles [https://edition.cnn.com/2021/03/31/health/pfizer-vaccine-manufacturing/index.html]. More specifically, this method is interesting because it enables the production of small and homogeneous liposomes (< 200 nm), compatible with sterile filtration with no requirement for specific equipment for liposome downsizing and no requirement for a lipid drying step to form a thin lipid film upstream of the process, a step that could be difficult to scale-up[26]. Manufacturing of SPA14 by "ethanol injection" was made possible by the high solubility of all its components in ethanol, including the TLR4 agonist E6020. For QS21 incorporation, two options were possible: upfront solubilization in ethanol with liposomal co-lipids or incorporation by post-addition to preformed E6020-liposomes, which is made possible by the high affinity of QS21 for the cholesterol-containing E6020-Liposomes[12,13]. Note that MPLA would not be compatible with this liposome manufacturing process due to the poor solubility of MPLA in ethanol. After composition adjustment and formulation buffer selection through an accelerated heat stability study, the immunological profiling of SPA14 was performed in vitro on human cells using the PTE module of the MIMIC® system and in vivo in both mice and NHPs using Sanofi's CMV vaccine candidate as a model antigen and AS01B as a comparator.

We found that the TLR4 agonist in SPA14, E6020, could activate human dendritic cells (DCs) very effectively at 10-100-fold lower concentrations than MPLA in the PTE module of the MIMIC® system, confirming previous observations made in standard PBMC assays[22]. We believe that the increased human cell stimulation capacity of E6020 over MPLA must be linked to the specific nature of the molecule and to a difference in signaling induced by a pure human TLR4 agonist (E6020) versus a mixture of human TLR4 agonists and antagonists (MPLA and MPL®) as demonstrated previously[9]. Our data also showed that the two TLR4 agonists, E6020 and MPLA, induced cytokine secretion by signaling through both MyD88 and TRIF-related pathways based on the induction of chemokines and cytokines related to the stimulation of both pathways[49]. Similar observations were made by Richard K. et al. (2020) who compared E6020 to a synthetic MPLA analogue[18]. In the MIMIC® PTE module, SPA14-20 induced higher expression of activation markers and cytokine secretions than AS01B, which was essentially driven by the highly active E6020 agonist in this assay. When compared to unformulated TLR4 agonists, SPA14 and AS01B displayed a reduced immunostimulatory effect in MIMIC®, indicating that the liposomal vehicle could attenuate the in vitro immunostimulatory capacity of the two TLR4 agonists. For instance, we did not detect IP-10 secretion induced by SPA14 and AS01B, whereas both E6020 and MPLA, as well as LPS + R848 control induced the secretion of this chemokine. Notably, concerning AS01, this effect could partly be due to potential differences in species composition between the research-grade MPLA employed as a standalone test article in the MIMIC® analysis and the GMP-grade MPL® in AS01B[9]. Overall, the liposomal vehicle (DOPC/Cholesterol + QS21) triggered minimal innate immune activation in the MIMIC® PTE

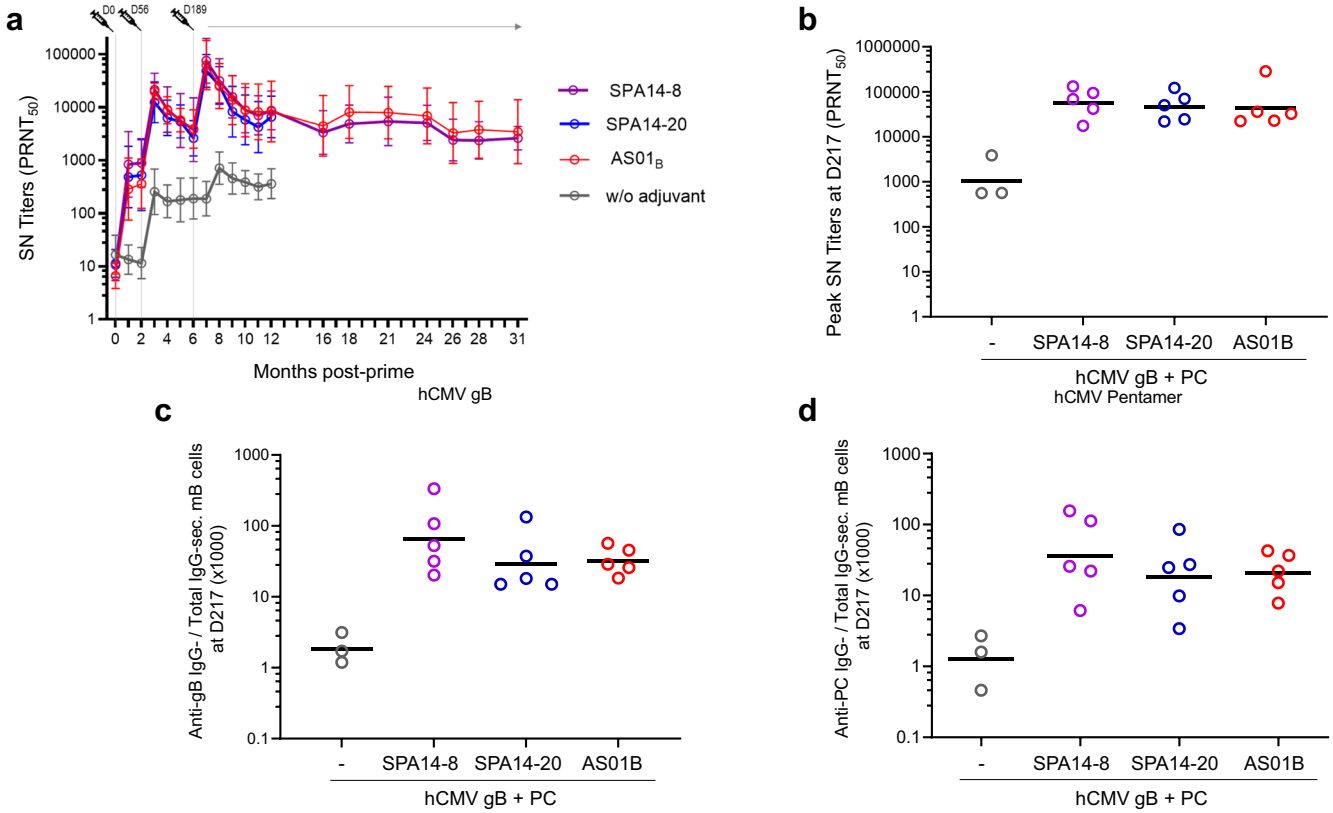

Fig. 7 | Serum neutralizing antibody response to hCMV virus and hCMV antigen specific IgG-secreting memory B cells measured in PBMC of the immunized NHPs. a BADrUL131-Y4 CMV virus strain neutralizing titers ($PRNT_{50}$) were determined using epithelial ARPE-19 cells and represented over time as group geometric means. **b** Individual neutralizing titers at the peak of antibody response (D217; 3 weeks following the boost) are shown as scattered plots with group GMTs (horizontal bars). **c** Individual (scattered plots) and group GMTs (horizontal bars) of CMV-gB-specific B cells over total IgG secreting B cells. **d** Individual (scattered plots) and group GMTs (horizontal bars) of CMV-PC-specific B cells over total IgG secreting B cells. Groups of macaques immunized with 20 µg of CMV-gB + 20 µg of CMV-PC in the absence of adjuvant (○), in the presence of SPA14-8 (○), SPA14-20 (○) or AS01B (○) are shown. Group comparisons were done by Tukey adjustment and one-way ANOVA but no significant difference was found between the adjuvanted groups.

module and reduced the immune activity and cytotoxicity of the TLR4 agonists. Similar observations had already been reported for MPLA when formulated into liposomes[50].

Overall, SPA14-8, SPA14-20 and AS01B all induced APC maturation in the MIMIC® PTE module but the levels of MyD88-related cytokines/chemokines induced by SPA14-20 were typically 5- to 20-fold higher and the levels of TRIF-related MCP-1, RANTES and IP-10 were typically 2- to 3 fold higher for SPA14-20 compared to SPA14-8 and AS01B. Interestingly, the increased in vitro immunostimulatory capacity of SPA14-20 over SPA14-8 and AS01B in MIMIC® did not translate into an increased adjuvant effect in the cynomolgus macaques, where the three adjuvants were compared (Figs. 7 and 8). This may be due to some specific difference between the human and macaque TLR4[51], and/or to suboptimal dosing in the macaques. Alternatively, the assessment of the adjuvant effects of SPA14 and AS01B via the biomarkers used in our macaque study may be dominated by QS21 effects. The dissection of the mechanism of action of SPA14 and the role of each of its components in the induced adjuvant effects would require more work and is the current focus in our group. Although this work is still underway, preliminary results indicate that SPA14 is significantly more effective than E6020-Liposomes (SPA14 lacking QS21) at inducing neutralizing antibody responses and more effective than QS21-Liposomes (SPA14 lacking E6020) at inducing CD4 + T cell responses with CMV-gB +PC in mice.

When tested in vivo with human cytomegalovirus gB and PC as test antigens, SPA14 was found to be as potent as AS01B at inducing CMV-neutralizing responses in mice and NHPs. Both adjuvants promoted the induction of strong neutralizing antibody titers and the induction of Th-1 responses based on IgG2c production in mice and IFN-γ production in mice and NHPs, but in mice, a higher level of Th-2 cytokines (IL-5) and higher IgG1 over IgG2c secreting cells ratios were obtained with SPA14 indicating that the Th-1 adjuvant profile of SPA14 could be less pronounced than that of AS01B. A similar trend was observed when the two adjuvants were compared by using split virus- and recombinant protein-based influenza vaccines in BALB/c mice[52]. This observation is likely linked to a specific feature of the QS21/E6020 combination, which also behaved differently from the QS21/MPL® combination (AS01B) in vitro, in the MIMIC® PTE module.

Concerning human CMV vaccine, previous clinical trials have shown that an MF59-adjuvanted CMV-gB vaccine could protect against primary CMV infection in young mothers although the duration of the induced antibody responses was deemed insufficient to afford protection in a congenital CMV infection setting[53,54]. With the inclusion of CMV-PC, which is the main target of neutralizing antibodies in hCMV seropositive individuals[55], and the use of a stronger adjuvant than MF59, the CMV-gB+PC/SPA14 vaccine candidate described in this report has the potential to significantly improve clinical efficacy. Especially, concerning antibody response durability, the frequencies of memory B cells and the longevity of the CMV neutralizing responses measured in mice and NHPs immunized with the CMV-gB+PC/SPA14 candidate vaccine support the induction of long-lasting protective immunity. Moreover, since SPA14 has been shown to be an effective adjuvant when used with different protein antigens in preclinical models[52], one could expect SPA14 to be useful for a broad range of human vaccines. This expectation is further supported by the effectiveness of yet other adjuvant

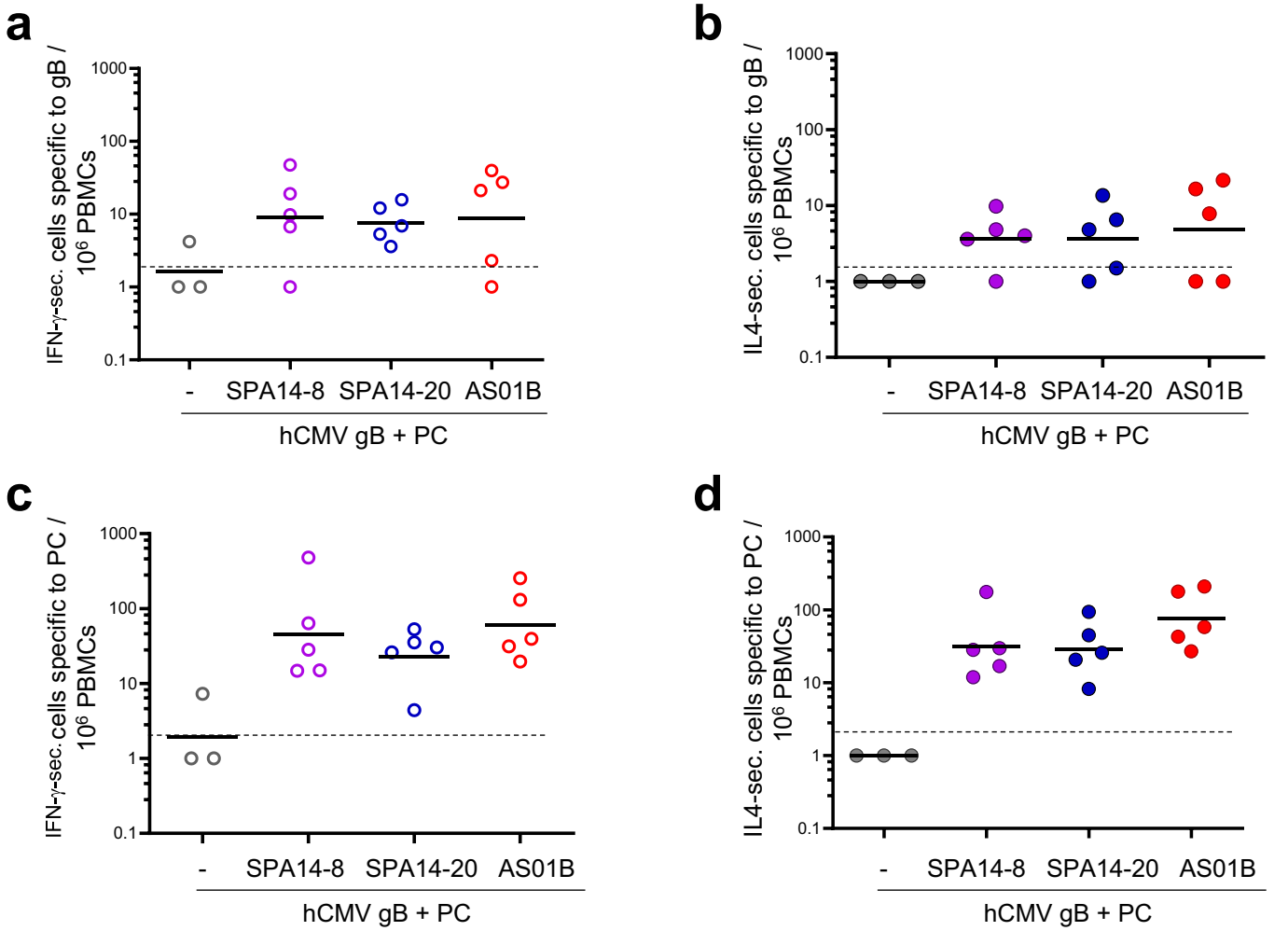

Fig. 8 | hCMV antigen specific IFN-γ- and IL-4-secreting cells measured in PBMCs of immunized NHP 9 days following the booster administration (D197). **a–d** From the immunized NHPs of Fig. 7, IFN-γ (**a, c**) and IL-4-secreting cells (**b, d**) specific to CMV gB and PC were measured in PBMCs by T cell ELISPOT at the peak of circulating T cell response on D197. For each NHP, the number of gB-specific IFN-γ or IL-4-secreting cells and the number of PC- specific IFN-γ- and IL-4-secreting cells per 10^6 PBMCs were represented as scattered plots with group GMTs (horizontal bars). Groups of macaques immunized in the absence of adjuvant (○,●), in the presence of SPA14-8 (○,●), SPA14-20 (○,●) or AS01B (○,●) are shown. Group comparisons were done by Tukey adjustment and one-way ANOVA but no significant differences were found between the adjuvanted groups.

systems combining a saponin with TLR4 agonists that were recently described[56,57].

In conclusion, this report describes a novel saponin-based liposomal adjuvant, termed SPA14, which combines QS21 with E6020 in cholesterol-containing liposomes. SPA14 is interesting from a product development perspective since it uses a well-defined fully synthetic single-entity TLR4 agonist, E6020, that is compatible with a readily scalable liposome manufacturing process by ethanol injection. Comparison of SPA14 against AS01B, indicated that each TLR4 agonist/QS21 combination could have a specific immunomodulatory profile, as suggested by the immunoprofiling in mice, NHPs and MIMIC®PTE module. In the present study, SPA14 appeared as a potent adjuvant for a CMV vaccine candidate comprising CMV gB plus PC, but overall, we believe that SPA14 could be broadly applicable to increase both CD4 T helper and B cell responses to a variety of protein vaccines. From a product stability perspective, SPA14 could be stored at 4 °C, separated from the antigens, as a long term stable ready-to-mix liquid adjuvant formulation, or combined with antigens in a single vial/syringe presentation (Hickey J.M. *et al.* Two recombinant cytomegalovirus antigens formulated with the SPA14 adjuvant system: Impact of temperature, pH and excipients on the stability of each antigen and adjuvant component. *Submitted for publication*).

Methods

Raw materials/formulation ingredients

GMP-grade E6020 was obtained from Eisai Inc. (Cambridge, MA). Highly purified QS21 was obtained from Desert King (San Diego, CA). Dioleoylphosphatidylcholine (>99% pure synthetic DOPC) and Cholesterol (>99% pure plant-derived cholesterol) were obtained from Avanti Polar Lipids (Alabaster, AL). Monophosphoryl lipid A from *Salmonella minnesota* R595 (MPLA) was obtained from InVivogen (MPLA-SM VacciGrade™; cat # vac-mpla) and from Sigma (cat # L6895). *Pseudomonas aeruginosa* lipopolysaccharide (LPS) and a synthetic TLR7/8 agonist (R848) used as an assay control in the MIMIC® PTE module were obtained respectively from Sigma (cat # L8643) and InVivogen (cat # TLRL-R848). AS01B was retrieved from commercial packages of Shingrix® (GSK) and comprised 100 µg/mL of MPL®, 100 µg/mL of QS21, 2 mg/mL of DOPC and 0.5 mg/mL of cholesterol in phosphate-buffered saline (PBS), pH 6.1.

Model vaccine antigens

Recombinant CMV-gB and CMV-PC were expressed in Chinese hamster ovary (CHO) cells. The CMV-gB (Towne strain) was expressed as a glycoprotein deleted from its transmembrane domain to enable secretion from the CHO cells. The CMV-PC, i.e., gH/gL/pUL128/pUL130/pUL131

(BE/28/2011 strain), was obtained as a secreted glycoprotein complex by transfection of CHO cells with 5 plasmids, each plasmid coding for one of the 5 proteins constituting the CMV PC. Glycoprotein H (gH) was deleted from its transmembrane domain to enable secretion of the PC[58]. CMV-gB and CMV-PC were purified to ≥ 99% as assessed by SDS PAGE, by using affinity chromatography and size exclusion chromatography, respectively. Endotoxin content in the recombinant antigens assessed by using the limulus amoebocyte assay (BioWhittaker Inc., Walkersville, MD) was less than 0.05 EU of LPS/mg of protein.

Determination of E6020 and MPLA solubility in ethanol

The solubility of E6020 and MPLA (Sigma) in ethanol was determined by using nephelometry to follow opalescence due to insolubility. The products were resuspended at 0.5, 1.0, 2.0 and 10 mg/mL in absolute ethanol (Carlo Erba). One mL of each suspension was stirred for 3 h at room temperature. Nephelometry was performed on a BMG-Labtech Nephelostar with 0.200 mL samples on a UV 96-well microplate (Thermo UV Flat Bottom 96; Ref. 8404) with an absolute ethanol blank.

Preparation and characterization of liposomal adjuvants

SPA14-20, SPA14-8, and the QS21-Liposomes were prepared by an ethanol injection technique as follows. Typically, a stock solution of QS21 at 1.0 mg/mL in CBS (10 mM citrate buffer, 140 mM NaCl, pH 6.3) was prepared by resuspending 3.0 mg of QS21 powder into 3.0 mL of CBS and sterile filtration on a 25 mm Pall Acrodisc® 0.2 µm membrane. A stock solution of E6020 at 2.0 mg/mL in ethanol was prepared by dissolving 2.0 mg of E6020 powder in 0.998 mL of ethanol. A fourfold concentrated stock solution of liposomal lipids in ethanol at 40 mg/mL of DOPC, 10 mg/mL of cholesterol and 0.2 mg/mL of E6020 was prepared by dissolving 40 mg of DOPC and 10 mg of cholesterol in 0.850 mL of ethanol and adding 0.100 mL of the E6020 stock solution. For the preparation of E6020-Liposomes, 1.0 mL of the liposomal lipid solution was injected into 3.0 mL of CBS under stirring at 1000 rpm, at room temperature, by using a Hamilton syringe with a 22-gauge needle and a syringe pump at 0.1 mL/min. E6020-Liposomes were dialyzed using Slide-A-Lyzer™ 10 K MWCO dialysis cassettes (Thermo Fischer Scientific, Courtaboeuf, France) three times (half a day, overnight and one full day) against CBS pH 6.3 to remove ethanol, sterile filtered on 33 mm Millex-GV PVDF 0.22 µm filters (Merck-Millipore), and stored at +4 °C under nitrogen until used. At this stage, E6020-Liposome components concentration was estimated according to the dilution factor of dialysis. For a typical 1.6 dilution factor, the liposomes composition was 6.25 mg/mL of DOPC, 1.56 mg/mL of Chol, and 0.031 mg/mL of E6020. SPA14 was prepared in sterile conditions by addition of 1.563 mL of the QS21 stock solution and 1.250 mL of CBS pH 6.3 to 5.0 mL of E6020-Liposomes. Under these conditions, the final concentration of SPA14 components was 4 mg/mL DOPC, 1 mg/mL Chol, 0.02 mg/mL E6020, and 0.2 mg/mL QS21. The mixture was vortexed for 10 s and stored at +4 °C under nitrogen. This preparation was termed SPA14-20 (20 referring to the E6020 content in µg/mL). SPA14-8 with a lower E6020 content (8 µg/mL) was prepared by following the same procedure but starting with a 0.8 mg/mL stock solution of E6020 in ethanol. QS21-Liposomes were prepared as described for SPA14 without including E6020 in the starting lipid solution in ethanol.

Liposome characterization

Size measurements. Liposome size (z-Average) was determined by dynamic light scattering (DLS) using the Malvern Zetasizer NanoZS (Malvern, Worcestershire, UK).

Electron microscopy of SPA14. SPA14 was visualized by cryo-transmission electron microscopy (cryo-TEM). A 4 µL sample was deposited on Quantifoil R2/2 cupper 200mesh grids (Quantifoil Instruments GmbH, Germany) after 90 s of glow discharge on an ELMO ionizer (Cordouan, France). Grids were blotted and frozen using a Vitrobot MARK IV (Thermo Scientific) and transferred for observation onto a TEM Tecnai-G20 (Thermo Scientific) operated at 200 kV using a 910 cryo-holder (Gatan Inc., USA). Images were recorded at 3 µm defocus and at low-dose mode (electron doses ≤ 10 $e^-/Å^2$) using an ssCCD Ultrascan 4000 (Gatan Inc., USA). Pixel size of recorded images was estimated to 0.221 nm after TEM calibration using a cross-line grid (EMS, USA) with pitch spacing of 500 nm and 2000 lines/mm.

HPLC determination of E6020 and QS21 content and integrity in SPA14. E6020 was determined and analyzed by HILIC HPLC/MS/MS as previously described[22] after solubilization of SPA14 in isopropanol/hexane/methanol 64:16:20 (v/v/v). QS21 was determined and analyzed by RP-HPLC (Agilent 1200 series) according to Brunner et al[59]. In brief, the separation and analysis of QS21 was performed by using an Hypersil Gold C4 column, 5 µm, 4.6 ×250 mm (Thermo Fisher Scientific; Ref. 25505-254630) maintained at 30 °C and eluted with a discontinuous acetonitrile gradient at a flow rate of 1 mL/min. The mobile phase was degassed by ultrasonic bath and consisted of 0.1% TFA in water in line A and 0.1% TFA in acetonitrile in line B. The gradient was as follows: T0: 30% B, T20 min: 55% B, T21 min: 30% B, T25 min: 30% B. The UV detector was set at 214 nm. Chromelon® 7.2 (Thermo Fisher Scientific) was used to process the data.

Hemolysis assay. The assay was performed in round bottom 96-well plates (Corning, cat#353077) using sheep red blood cells (RBCs) obtained from Rockland (Pennsylvania, PA; Ref. R405-0050). Before use, the RBCs (5 mL in a 15 mL Falcon tube) were washed twice with cold PBS by centrifugation at 4 °C for 10 min at 700 g and resuspended in 5 mL of PBS. Next, 100 µL of PBS, 100 µL of test item (QS21 in twofold serial dilutions from 200 to 1.6 µM in CBS pH 6.3) and 25 µL of the RBC suspension were subsequently added into the microwells of the 96-well plate. After 30 min of incubation at 37 °C, the plates were centrifuged for 5 min at 700 g at room temperature and 80 µL of well supernatants were transferred into a flat bottom 96-well plate (Corning, cat#3599) for absorbance reading at 540 nm using a plate reader (VersaMax – Molecular Devices). The percentage of cell hemolysis was calculated according to the formula: 100 x [(sample absorbance - negative control absorbance) / (positive control absorbance - negative control absorbance)]. Negative and positive controls were obtained by replacing the test item with plain CBS or distilled water, respectively.

Immunological studies

Statements of ethics. Animal study protocols were reviewed by Sanofi Ethics Committee (Marcy L'Etoile, France). The macaque study was included in the project number APAFIS#16801–2018092011168040 v2 and the mouse studies in the project AFAPIS#16508–2018081313297024 v1, both approved by the French Ministry of Higher Education, Research and Innovation (MHERI). All experiments were conducted in accordance with the European Directive 2010/63/UE as published in the French Official Journal of February 7th, 2013. Mice and monkeys were housed in animal care facilities accredited by the Association for Assessment and Accreditation of Laboratory Animal Care (AAALAC).

Profiling the adjuvants by using the PTE module of the MIMIC® system

PBMC preparation. Apheresis blood products were collected from donors at OneBlood (Orlando, FL). The study protocol and donor program were reviewed and approved by Chesapeake Research Review, Inc. (Columbia, MD). At the time of collection, peripheral blood mononuclear cells (PBMCs) from healthy donors were enriched by Ficoll density gradient separation and cryopreserved in DMSO-containing freezing media.

MIMIC® PTE assay. The MIMIC® PTE construct was assembled on a robotic line using published methods[27,33,34]. Briefly, endothelial cells were grown to confluence atop a collagen matrix (Advanced Biomatrix, San Diego, CA). Thereafter, donor PBMCs prepared from frozen stocks were applied to the assay wells. After an incubation of 90 min, non-migrated cells were removed by washing and treatments were added to the cultures at different dilutions. A mixture of 100 ng/mL LPS and 10 µg/mL R848 was used as a positive control in these assays. This study, evaluating the ability of SPA14 and AS01B to stimulate human immune cells, was designed to test two concentrations of E6020 in SPA14, i.e., 8 and 20 µg/mL, keeping constant all other SPA14 ingredients. Test items were diluted 1:20 to 1:160 in a 2-fold dose curve. To understand the contribution of the QS21-liposomes to the innate immune signature induced by SPA14 or AS01B, QS21-liposomes (minus any TLR4 agonist) were also examined at the 1:40 dilution. E6020, the TLR4 agonist in SPA14, was also dosed alone in the assay at a concentration of 200 ng/mL (corresponding to the 1:40 dilution of the SPA14 dose range) and can be compared to MPLA (InvivoGen) at 5 µg/mL (corresponding to the 1:20 dilution of the AS01B dose range). Cells and culture supernatants were harvested after a 48-hr treatment period. The culture supernatants were analyzed for cytokines/chemokines using the Milliplex® human 12-plex multi-cytokine detection system (Millipore) based on the manufacturer protocol. The kit included IFN-α2, IFNγ, IL-1β, IL-6, IL-8, IL-10, IL-12p40, IP-10, MCP-1, MIP-1β, RANTES, and TNFα. PGE2 secretion was evaluated by ELISA following the manufacturer's protocol (Arbor assay, MI, cat # K051-H5, MI). The cells were phenotyped using various markers by flow cytometry. Data were exported to GraphPad Prism (GraphPad Software, San Diego, CA, USA) for graph preparation.

Cytokine secretion assay. Analyte concentrations were calculated based on relevant standard curves using the Bio-Plex® manager software. For run acceptance criteria, LLOQ and ULOQ for each analyte were established based on the percent recovery (Observed/Expected*100) of each point against a 5-parameter logistic (5PL) curve fit of the standard values. A recovery percentage of 80 - 120% was considered acceptable, such that values falling within this range were used to set the lower and upper bounds of the standard curve. The raw data file was reviewed for bead counts; a data point was considered valid when a minimum of 35 beads per region was counted.

Cellular phenotype by flow cytometry. MIMIC® PTE-derived cells were washed with PBS and labeled with Live-Dead Aqua (Thermo Fisher Scientific, USA) for 20 min on ice. After washing and performing an IgG-Fc block (Normal mouse serum; Cat # 015-000-120, Jackson Immuno Research Laboratories), the cells were incubated with a cocktail of fluorochrome-labeled monoclonal antibodies, such as anti-CD14, anti-HLA-DR, anti-CD11c, anti-CD86, anti-CD25, anti-CD3 and anti-CD19, that are specific for non-myeloid lineage cells and immune ligands (BD Biosciences, San Jose, CA). Thereafter, the cells were washed with buffered media and acquired on a BD Fortessa flow cytometer equipped with BD FACS Diva software (BD Biosciences). Data analysis was performed using FlowJo software (Tree Star, Ashland, OR). For flow gating, doublets were first excluded from the live-cell population and then lymphocytes (CD3 + , CD19 +) were removed from the analysis using a dump-channel approach. Next, HLA-DR+ cells were gated into CD11c+ monocytic DCs. Thereafter, mDC subpopulations were analyzed for their expression of HLA-DR and maturation/activation markers (CD14, CD86 and CD83) by Mean Fluorescent Intensity (MFI) and % of positive cells.

Preparation of experimental vaccine formulations for animal studies

The experimental vaccine formulations comprising CMV gB + PC were prepared by diluting and mixing concentrated antigen stock solutions, followed by the addition of the adjuvant. Specifically, for AS01B, 50 µl of an antigen mixture at 400 µg/mL of CMV-gB and 400 µg/mL of CMV-PC in PBS were added into 500 µL of AS01B (as retrieved from the Shingrix package). Mice and NHPs received 55 µL and 550 µL of vaccine formulation, respectively. The adjuvanted vaccine formulations were used within 3 h of preparation. In this way, monkeys in the AS01B group received 20 µg CMV-gB + 20 µg CMV-PC + 50 µg QS21 + 50 µg MPL®.

For SPA14-20 and SPA14-8, 250 µl of an antigen mixture at 80 µg/mL of CMV-gB and 80 µg/mL of CMV-PC in PBS were added to 250 µL of SPA14 (or to 250 µl of plain CBS in case of antigen alone group). Mice were immunized within 3 h with 50 µl and monkeys with 500 µl of the preparations. In this way, monkeys in the SPA14 groups received 20 µg CMV-gB + 20 µg CMV-PC + 50 µg QS21 + 5 µg or 2 µg E6020.

Immunization of mice

C57BL/6 J female mice (16 per group), aged 6–8 weeks (body weight 18–20 g) at the time of first immunization were obtained from Charles River Laboratories (Saint Germain sur l'Arbresle, France). Mice were immunized twice, 3 weeks apart (D0, D21), by intramuscular injection into the quadriceps. Immunization was performed under gaseous anesthesia with 5% isoflurane using a TEM SEGA gas anesthesia table for rodents. Blood samples were collected at different time points following immunization for the analysis of antibody responses (D20, D35, D91, D179) by ELISA and/or virus plaque reduction assays. Intermediate blood samplings were performed under 5% isoflurane gas anesthesia. Terminal blood samplings were performed under deep chemical anesthesia. Mice were injected by the intra-peritoneal route with 0.1 mL/10 g body weight of a Ketamine plus Xylazine mixture (80 mg/kg of Imalgène® 1000 + 16 mg/kg Rompun® 2%). After anesthesia, terminal blood sampling was performed by carotid section. After spleen collection, mice were euthanized by cervical dislocation.

Eight mice per group were euthanized at D35 and the remaining mice were euthanized at D179. Individual spleens were collected in a sterile 50 mL Falcon tube containing RPMI medium and mechanically dissociated using GentleMACS (Miltenyi Biotec). The tubes were centrifuged at 500 g for 10 min at 4 °C and the supernatants discarded. Spleen cell pellets were resuspended with 1 mL of red blood cell lysis buffer (Sigma; cat # R 7757) and gently mixed for 1 min. The lysis reaction was stopped by placing the tubes in crushed ice followed by an addition of 20 mL of cold RPMI medium. The tubes were then centrifuged at 500 g for 7 min and the supernatants discarded. Spleen cell pellets were resuspended in RPMI containing 10% fetal calf serum (FCS) and prepared for cell counting before use in B and T cell ELISPOT assays using Fluorospot kits described below.

Immunization of NHPs (macaques)

Groups of 5 male cynomolgus macaques (2.4–3.5 kg body weight) obtained from Noveprim (Camarney, Spain) were housed in collective cages based on social affinity under controlled humidity, temperature, and light (12-hour light/12-hour dark cycles) and allowed to acclimatize for 4 weeks before study procedures. The macaques were monitored and fed 1–2-times daily with commercial monkey chow and fruits, and water *ad libitum*. Environmental enrichment provided included toys, novel foodstuffs, and music. They were immunized twice 8 weeks apart (D0, D56) and boosted 6 months later (D189) with 500 µL of the vaccine formulations by intramuscular injection into the upper arm deltoid muscle. Blood samples were collected pre-immunization (D-8) and at different time points following immunization (D28, D55, D84, D118, D168, D181, D217, D237, D273, D300, D331, D357 and then every 2-3 months over a 1.5-year follow-up period). For experimental procedures such as animal handling, weighing injection point observation, animals were trained during the acclimatization period and these procedures were conducted with conscious animals. Immunizations and blood sampling were conducted after mild sedation using ketamine hydrochloride (Imalgene 1000, Boehringer, 10 mg/kg, intramuscular route). Blood and serum samples were used for the analysis of virus-neutralizing antibody responses by plaque reduction assay, and specific T cell

responses (D197, 8 days post-boosting) and memory B cell responses (D217, four weeks postboosting) by ELISPOT. For ELISPOT assays, blood was collected in Sodium-Heparin tubes (Becton-Dickinson Vacutainer®; Ref. 267876) for PBMC isolation. PBMCs were stored frozen in liquid nitrogen until analysis. Clinical observations, including temperature and injection site observation, were performed over three days after each injection. Animals body weight was also monitored all along the study.

Determination of binding antibody titers in mouse serum

Serum antibodies directed against CMV gB or PC were titrated by ELISA. In brief, Dynex 96-well microplates were coated overnight at 4 °C with 100 µL of CMV-gB (1 µg/mL) or CMV-PC (2 µg/mL), in 0.05 M carbonate/ bicarbonate buffer, pH 9.6 (Sigma). Next, plates were blocked for at least 1 h at 37 °C with 150 µL/well of PBS-Tween-milk (PBS pH 7.1, 0.05% Tween 20, 1% (w/v) powdered skim milk (DIFCO). All subsequent incubations were carried out in a final volume of 100 µL, each followed by 3 washes with PBS-Tween. Two-fold serial dilutions of serum samples were performed in PBS-Tween-milk (starting from 1/100, 1/1000 or 1/10000) and were added to the wells. Plates were incubated for 90 min at 37 °C. After washing, goat anti-mouse IgG1- or IgG2c-HRP (Southern Biotech, cat# 1070-05 and 1079-05, respectively) diluted in PBS-Tween-milk at 1/2000 were added to the wells. Plates were incubated for 90 min at 37 °C, washed and further incubated in the dark for 30 min at room temperature with 100 µL/well of a ready-to-use Tetra Methyl Benzidine (TMB) substrate solution (TEBU, cat# TMBW1000-01). The reaction was stopped with 100 µL/well of HCl 1 M (Prolabo, cat# 30024290). Optical density (OD) was measured at 450 nm-650 nm with a plate reader (VersaMax – Molecular Devices). Specific antibody titers were determined using the CodUnit software, for an OD value range of 0.2 to 3.0 from the titration curve (reference mouse hyperimmune serum put on each plate). The titer of the references, expressed in arbitrary ELISA units (EU), was previously calculated as the reciprocal dilution giving an OD of 1.0. The threshold of antibody detection was 10 EU (1.0 log10).

Determination of neutralizing antibody titers

Neutralizing antibodies in sera from immunized mice and macaques were titrated using a plaque reduction seroneutralization assay on ARPE-19 epithelial cells and on MRC-5 fibroblasts as described previously[60].

Specific CMV-gB and PC memory B cell frequencies in mice and NHPs

For the NHP study, PBMCs were isolated from whole blood collected into Vacutainer tubes with sodium heparin (Becton Dickenson) at regular time points. Whole blood was diluted to 1:3 in PBS and 30 ml of diluted whole blood layered over 15 mL of Lymphoprep 95% (Stemcell). After centrifugation, the buffy coat was harvested and washed with RPMI + 10% FBS. Splenocytes (for mouse studies) or PBMCs (for NHP studies) were counted using a Muse cell counter. Fresh PBMCs or mouse splenocytes were plated for 3 days in 6-well culture plates in RPMI medium plus R848 (1 µg/mL) and IL-2 (10 ng/mL).

For NHP studies, CMV-gB and CMV-PC specific memory B cell ELISPOT were performed using a commercial kit from Mabtech (Human IgG/IgM Fluorospot kit, cat # FS-05R17G-10). Multiscreen™ 96-well IPFL plates (Mabtech; Ref. 3654-FL-10) were pre-wetted with 25 µL of 35% ethanol for 1 min, washed with PBS and coated overnight at 5 °C with 100 µL/well of either CMV-gB, CMV-PC (10 µg/mL) or anti-IgG or -IgM antibodies from Mabtech (15 µg/mL). Next, the plates were washed with PBS and blocked for 2 h at 37 °C with RPMI containing 10% FBS, 200 mM L-Glutamine, 100 U/mL penicillin, and 10 µg/mL streptomycin. After washing with PBS, $4x10^5$ R848 plus IL-2 treated PBMCs from immunized NHPs were plated per well and incubated for 5 h at 37 °C in a 5% CO2 incubator. After 6 washes in PBS-0.5% BSA, the plates were incubated for 2 h at 37 °C with 100 µL/well of anti-human IgG-Cy3 conjugate (Mabtech; cat # MT78/145), and anti-human IgM-FITC conjugate (Mabtech; cat # MT22). After extensive washing with PBS, fluorescent spots were enumerated with an automated spot reader equipped with filters for Cy3 and FITC (Microvision Instruments, Evry, France). The same protocol was used for mouse studies, with anti-mouse antibodies: goat anti-mouse total IgG (KPL, cat#01-18-02), goat anti-mouse IgG1-PE conjugate (Southern biotech; cat # 1070-09), goat anti-mouse IgG2c-FITC conjugate (Southern biotech; cat # 1079-02), goat anti-mouse IgG-PE conjugate (Southern biotech; cat # 1032-09).

Determination of IFN-γ / IL-5 (mouse) or IFN-γ / IL-4 (NHP) secreting T cells specific to CMV-gB and CMV-PC

Mouse and NHP Fluorospot kits were purchased from Mabtech (cat # FS-4143-10 for mouse and Fluorospot flex for NHP). Multiscreen™ 96-well IPFL plates were prepared as described above for the B cell assay and coated overnight at 5 °C with 100 µL/well of rat anti-mouse IFN-γ or rat anti-mouse IL-5 mAb (15 µg/mL). Next, the plates were washed with PBS and blocked for 2 h at 37 °C with RPMI containing 10% FBS, 200 mM L-Glutamine, 100 U/mL penicillin and 10 µg/mL streptomycin. After washing with PBS, $5×10^5$ freshly isolated spleen cells (mice) or PBMCs (NHPs) were added per well and incubated for 24 h with CMV-gB (0.1 µg/mL), CMV-PC (0.1 µg/mL), medium alone as negative control or concanavalin A (2.5 µg/mL) as a positive control. After 6 washes with 0.1% bovine serum albumin (BSA) in PBS (200 µL per well), anti-mouse or NHP IFN-γ BAM-conjugated or biotinylated anti-mouse IL-5 or anti-NHP IL-4 antibodies at 2 µg/ml in PBS-0.1% BSA were added (100 µL per well) and incubated for 2 h at room temperature in the dark. After 6 washes in PBS-0.1% BSA, 100 µL of streptavidin-Cy3 conjugate or FITC conjugated anti-BAM antibody (1/200 dilution) in PBS-0.1% BSA were added per well and incubated for 2 h in the dark. After 6 washes with PBS-0.1% BSA, fluorescent spots were enumerated with an automated spot reader equipped with a filter for PE fluorescence (Microvision). Results were expressed as number of specific IFN-γ-, IL-5- or IL-4-secreting cells per 10^6 cells after subtracting fluorospot counts from negative control wells.

Statistical analyses

For the MIMIC® PTE study, statistical analysis was performed by unpaired, two-tailed t-test for relevant conditions using GraphPad Prism version 10.1.2. For the cytokine heatmap analysis, geometric mean values were calculated for all donors, treatment, and analytes. The heatmap was made in R studio Version 4.1.2 with heatmap package [https://cran.r-project.org/package=pheatmap] using log2 (fold change) values relative to geometric mean values. The heatmap package was downloaded from the Comprehensive R Archive Network (CRAN) repository. For certain comparisons, one-way ANOVA with Tukey post-tests (GraphPad Prism) were performed, with $p < 0.05$ being considered statistically significant. For mouse and NHP studies, group comparisons were performed using one- or two-way or repeated ANOVA as a function of the readout on SAS v9.2 (SAS Institute, Cary, NC). For data with several timepoints (i.e., antibody responses over time) an ANOVA from a mixed model with group, time and their interaction was applied. The type of covariance structure used in the model was decided based on the lowest AIC criterion obtained. To account for multiple testing, a Dunnett or Tukey adjustment was applied for group comparisons.

Computer code and algorithm

The heatmap was made in R studio Version 4.1.2 with heatmap package [https://cran.r-project.org/package=pheatmap].

Data availability

The data generated and/or analyzed during the study are available from the corresponding author upon reasonable request.

Received: 12 January 2024; Accepted: 6 December 2024;
Published online: 19 December 2024

References

1. Pulendran, B., Arunachalam, P. S. & O'Hagan, D. T. Emerging concepts in the science of vaccine adjuvants. *Nat. Rev. Drug Discov.* **20**, 454–475 (2021).
2. Kensil, C. R. & Kammer, R. QS-21: a water-soluble triterpene glycoside adjuvant. *Expert Opin. Investig. Drugs* **7**, 1475–1482 (1998).
3. Lacaille-Dubois, M. A. Updated insights into the mechanism of action and clinical profile of the immunoadjuvant QS-21: A review. *Phytomedicine* **60**, 152905 (2019).
4. Ishizaka, S. T. & Hawkins, L. D. E6020: a synthetic Toll-like receptor 4 agonist as a vaccine adjuvant. *Expert Rev. Vaccines* **6**, 773–784 (2007).
5. McGirr, A. et al. The comparative efficacy and safety of herpes zoster vaccines: A network meta-analysis. *Vaccine* **37**, 2896–2909 (2019).
6. Ulrich, J. T. & Myers, K. R. Monophosphoryl lipid A as an adjuvant. Past experiences and new directions. *Pharm. Biotechnol.* **6**, 495–524 (1995).
7. Evans, J. T. et al. Enhancement of antigen-specific immunity via the TLR4 ligands MPL adjuvant and Ribi.529. *Expert Rev. Vaccines* **2**, 219–229 (2003).
8. Fox, C. B., Friede, M., Reed, S. G. & Ireton, G. C. Synthetic and natural TLR4 agonists as safe and effective vaccine adjuvants. *Subcell. Biochem* **53**, 303–321 (2010).
9. Wang, Y. Q., Bazin-Lee, H., Evans, J. T., Casella, C. R. & Mitchell, T. C. MPL Adjuvant Contains Competitive Antagonists of Human TLR4. *Front Immunol.* **11**, 577823 (2020).
10. Didierlaurent, A. M. et al. In Immunopotentiators in Modern Vaccines (Second Edition) (eds Schijns V. E. J. C. & O'Hagan D. T.) 265-285 (Academic Press, 2017).
11. Didierlaurent, A. M. et al. Adjuvant system AS01: helping to overcome the challenges of modern vaccines. *Expert Rev. Vaccines* **16**, 55–63 (2017).
12. Beck, Z., Matyas, G. R. & Alving, C. R. Detection of liposomal cholesterol and monophosphoryl lipid A by QS-21 saponin and Limulus polyphemus amebocyte lysate. *Biochim Biophys. Acta* **1848**, 775–780 (2015).
13. Garçon, N. & Di Pasquale, A. From discovery to licensure, the Adjuvant System story. *Hum. Vaccin Immunother.* **13**, 19–33 (2017).
14. Kester, K. E. et al. Randomized, double-blind, phase 2a trial of falciparum malaria vaccines RTS,S/AS01B and RTS,S/AS02A in malaria-naive adults: safety, efficacy, and immunologic associates of protection. *J. Infect. Dis.* **200**, 337–346 (2009).
15. Agnandji, S. T., Fernandes, J. F., Bache, E. B. & Ramharter, M. Clinical development of RTS,S/AS malaria vaccine: a systematic review of clinical Phase I-III trials. *Future Microbiol* **10**, 1553–1578 (2015).
16. Seydel, U. et al. The generalized endotoxic principle. *Eur. J. Immunol.* **33**, 1586–1592 (2003).
17. Hawkins, L. D. et al. A novel class of endotoxin receptor agonists with simplified structure, toll-like receptor 4-dependent immunostimulatory action, and adjuvant activity. *J. Pharm. Exp. Ther.* **300**, 655–661 (2002).
18. Richard, K. et al. Dissociation of TRIF bias and adjuvanticity. *Vaccine* **38**, 4298–4308 (2020).
19. Gopalakrishnan, A. et al. E6020, a TLR4 Agonist Adjuvant, Enhances Both Antibody Titers and Isotype Switching in Response to Immunization with Hapten-Protein Antigens and Is Diminished in Mice with TLR4 Signaling Insufficiency. *J. Immunol.* **209**, 1950–1959 (2022).
20. Morefield, G. L., Hawkins, L. D., Ishizaka, S. T., Kissner, T. L. & Ulrich, R. G. Synthetic Toll-like receptor 4 agonist enhances vaccine efficacy in an experimental model of toxic shock syndrome. *Clin. Vaccin. Immunol.* **14**, 1499–1504 (2007).
21. Singh, M. et al. MF59 oil-in-water emulsion in combination with a synthetic TLR4 agonist (E6020) is a potent adjuvant for a combination Meningococcus vaccine. *Hum. Vaccin Immunother.* **8**, 486–490 (2012).
22. Haensler, J. et al. Design and preclinical characterization of a novel vaccine adjuvant formulation consisting of a synthetic TLR4 agonist in a thermoreversible squalene emulsion. *Int J. Pharm.* **486**, 99–111 (2015).
23. Pollet, J. et al. A simple fluorescence-based assay for quantification of the Toll-Like Receptor agonist E6020 in vaccine formulations. *Vaccine* **35**, 1410–1416 (2017).
24. Batzri, S. & Korn, E. D. Single bilayer liposomes prepared without sonication. *Biochim Biophys. Acta* **298**, 1015–1019 (1973).
25. Wagner, A., Vorauer-Uhl, K., Kreismayr, G. & Katinger, H. The crossflow injection technique: an improvement of the ethanol injection method. *J. Liposome Res* **12**, 259–270 (2002).
26. Charcosset, C., Juban, A., Valour, J.-P., Urbaniak, S. & Fessi, H. Preparation of liposomes at large scale using the ethanol injection method: Effect of scale-up and injection devices. *Chem. Eng. Res. Des.* **94**, 508–515 (2015).
27. Ma, Y. et al. Assessing the immunopotency of Toll-like receptor agonists in an in vitro tissue-engineered immunological model. *Immunology* **130**, 374–387 (2010).
28. Cleland, J. L. et al. Isomerization and formulation stability of the vaccine adjuvant QS-21. *J. Pharm. Sci.* **85**, 22–28 (1996).
29. Hervé, C., Laupèze, B., Del Giudice, G., Didierlaurent, A. M. & Tavares Da Silva, F. The how's and what's of vaccine reactogenicity. *NPJ Vaccines* **4**, 39 (2019).
30. Burny, W. et al. Inflammatory parameters associated with systemic reactogenicity following vaccination with adjuvanted hepatitis B vaccines in humans. *Vaccine* **37**, 2004–2015 (2019).
31. Zaitseva, M. et al. Use of human MonoMac6 cells for development of in vitro assay predictive of adjuvant safety in vivo. *Vaccine* **30**, 4859–4865 (2012).
32. Won, S. J. & Lin, M. T. Pyrogenicity of polyadenylic.polyuridylic acid in rabbits. *Naunyn Schmiedebergs Arch. Pharm.* **343**, 551–557 (1991).
33. Luna, E. et al. Evaluation of the innate immunostimulatory potential of originator and non-originator copies of insulin glargine in an in vitro human immune model. *PLoS One* **13**, e0197478 (2018).
34. Luna, E. et al. Evaluation of Immunostimulatory Potential of Branded and US-Generic Enoxaparins in an In Vitro Human Immune System Model. *Clin. Appl Thromb. Hemost.* **21**, 211–222 (2015).
35. Syntin, P., Piras-Douce, F., Dalençon, F., Garinot, M. & Haensler, J. Nonclinical safety assessments of a novel synthetic toll-like receptor 4 agonist and saponin based adjuvant. *Toxicol. Appl Pharm.* **460**, 116358 (2023).
36. Collin, M., McGovern, N. & Haniffa, M. Human dendritic cell subsets. *Immunology* **140**, 22–30 (2013).
37. Kagan, J. C. et al. TRAM couples endocytosis of Toll-like receptor 4 to the induction of interferon-beta. *Nat. Immunol.* **9**, 361–368 (2008).
38. Mata-Haro, V. et al. The vaccine adjuvant monophosphoryl lipid A as a TRIF-biased agonist of TLR4. *Science* **316**, 1628–1632 (2007).
39. Chlibek, R. et al. Long-term immunogenicity and safety of an investigational herpes zoster subunit vaccine in older adults. *Vaccine* **34**, 863–868 (2016).
40. Leroux-Roels, I. et al. Safety and Immunogenicity of a Respiratory Syncytial Virus Prefusion F (RSVPreF3) Candidate Vaccine in Older Adults: Phase 1/2 Randomized Clinical Trial. *J. Infect. Dis.* **227**, 761–772 (2023).
41. Papi, A. et al. Respiratory Syncytial Virus Prefusion F Protein Vaccine in Older Adults. *N. Engl. J. Med* **388**, 595–608 (2023).
42. RTS S Clinical Trials Partnership. Efficacy and safety of RTS,S/AS01 malaria vaccine with or without a booster dose in infants and children in Africa: final results of a phase 3, individually randomised, controlled trial. *Lancet* **386**, 31–45 (2015).

43. Leroux-Roels, I. et al. Improved CD4$^+$ T cell responses to Mycobacterium tuberculosis in PPD-negative adults by M72/AS01 as compared to the M72/AS02 and Mtb72F/AS02 tuberculosis candidate vaccine formulations: a randomized trial. *Vaccine* **31**, 2196–2206 (2013).
44. Van Braeckel, E. et al. An adjuvanted polyprotein HIV-1 vaccine induces polyfunctional cross-reactive CD4+ T cell responses in seronegative volunteers. *Clin. Infect. Dis.* **52**, 522–531 (2011).
45. Plotkin, S. A. et al. The Status of Vaccine Development Against the Human Cytomegalovirus. *J. Infect. Dis.* **221**, S113–s122 (2020).
46. Van Hoeven, N. et al. A combination of TLR-4 agonist and saponin adjuvants increases antibody diversity and protective efficacy of a recombinant West Nile Virus antigen. *NPJ Vaccines* **3**, 39 (2018).
47. Alving, C. R., Peachman, K. K., Matyas, G. R., Rao, M. & Beck, Z. Army Liposome Formulation (ALF) family of vaccine adjuvants. *Expert Rev. Vaccines* **19**, 279–292 (2020).
48. Khan, M. S. et al. Enhancing immunogenicity of a thermostable, efficacious SARS-CoV-2 vaccine formulation through oligomerization and adjuvant choice. *Pharmaceutics* **15**, 2759 (2023).
49. Shen, H., Tesar, B. M., Walker, W. E. & Goldstein, D. R. Dual signaling of MyD88 and TRIF is critical for maximal TLR4-induced dendritic cell maturation. *J. Immunol.* **181**, 1849–1858 (2008).
50. Alving, C. R., Rao, M., Steers, N. J., Matyas, G. R. & Mayorov, A. V. Liposomes containing lipid A: an effective, safe, generic adjuvant system for synthetic vaccines. *Expert Rev. Vaccines* **11**, 733–744 (2012).
51. Vaure, C. & Liu, Y. A comparative review of toll-like receptor 4 expression and functionality in different animal species. *Front Immunol.* **5**, 316 (2014).
52. WO/2022/090359 – Liposomes containing TLR4 agonist, preparation and uses thereof.
53. Pass, R. F. et al. Vaccine prevention of maternal cytomegalovirus infection. *N. Engl. J. Med* **360**, 1191–1199 (2009).
54. Krause, P. R. et al. Priorities for CMV vaccine development. *Vaccine* **32**, 4–10 (2013).
55. Fouts, A. E., Chan, P., Stephan, J. P., Vandlen, R. & Feierbach, B. Antibodies against the gH/gL/UL128/UL130/UL131 complex comprise the majority of the anti-cytomegalovirus (anti-CMV) neutralizing antibody response in CMV hyperimmune globulin. *J. Virol.* **86**, 7444–7447 (2012).
56. Silva, M. et al. A particulate saponin/TLR agonist vaccine adjuvant alters lymph flow and modulates adaptive immunity. *Sci. Immunol.* **6**, eabf1152 (2021).
57. Ou, B. S. et al. Saponin Nanoparticle Adjuvants Incorporating Toll-Like Receptor Agonists Improve Vaccine Immunomodulation. *bioRxiv* https://doi.org/10.1101/2023.07.16.549249 (2023).
58. Hofmann, I. et al. Expression of the human cytomegalovirus pentamer complex for vaccine use in a CHO system. *Biotechnol. Bioeng.* **112**, 2505–2515 (2015).
59. Brunner, L., Barnier-Quer, C. & Collin, N. QS-21 Adjuvant: Laboratory-Scale Purification Method and Formulation Into Liposomes. *Methods Mol. Biol.* **1494**, 73–86 (2017).
60. Garinot, M. et al. A potent novel vaccine adjuvant based on straight polyacrylate. *Int J. Pharm. X* **2**, 100054 (2020).

Acknowledgements

We thank Cécile Verdelet, Anne Hervier, Franck Raynal, Sandrine Painchaud, Antonin Asmus and Julie Barrier (all from Sanofi/FR) for expert technical assistance and Julie Piolat (Sanofi/FR), Nada Assi (Sanofi/FR) and Ivan Ordonez (Sanofi/US) for their contributions to the statistical analyses. We thank Chelsea Fnu (Sanofi/US) for heat map and bioinformatic support. We thank Lucie Engelhart (Sanofi/FR) for animal care. We also thank Charles Lutsch (Sanofi/FR) for supporting this work, Jean-Sébastien Bolduc (Sanofi/FR) and Manojkumar Patel (Sanofi/IN) for editorial assistance, and Sanofi for funding of this work.

Author contributions

Conceptualization and methodology: E.L., S.R., M.G., F.P., D.R.D., B.R., D. L. and J.H. Investigations: P.A., C.C., J.E., L.R., M-J. A. Writing Original Draft: J.H. Review & Editing: E.L., S.R., M.G., F.P., D.R.D., B.R., F.G.F., D.L. and J.H. Supervision: D.R.D., B.R., D.L. and J.H.

Competing interests

All authors except F.G.F. are Sanofi employees or were under contract with Sanofi at the time of the study and may hold shares and/or stock options in the company. F.G.F. is an employee of Eisai and may hold shares and/or stock options in the company. The authors declare no other financial and non-financial competing interests.

Additional information

Supplementary information The online version contains supplementary material available at https://doi.org/10.1038/s41541-024-01046-0.

Correspondence and requests for materials should be addressed to Jean Haensler.